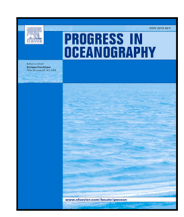
ELSEVIER

Contents lists available at ScienceDirect

Progress in Oceanography

journal homepage: www.elsevier.com/locate/pocean





Lifting the lid on Marine Heatwaves

Neil Malan a,b,, Alex Sen Gupta a,b,c,d, Amandine Schaeffer b,e, Shujing Zhang c,f, Martina A. Doblin g,h, Gabriela Semolini Pilo b, Andrew E. Kiss c,j, Jason D. Everett b,k, Erik Behrens b, Antonietta Capotondi b, Sophie Cravatte b, Alistair J. Hobday b, Neil J. Holbrook c,f, Jules B. Kajtar b, Claire M. Spillman b, Spillman b,

- ^a Climate Change Research Centre, University of New South Wales, Sydney, Australia
- ^b Centre for Marine Science and Innovation, University of New South Wales, Sydney, Australia
- ^c ARC Centre of Excellence for Climate Extremes, Australia
- ^d ARC Centre of Excellence for Antarctic Science, Australia
- e School of Mathematics and Statistics, University of New South Wales, Sydney, Australia
- f Institute for Marine and Antarctic Studies, University of Tasmania, Hobart, Tasmania, Australia
- ⁸ Climate Change Cluster, University of Technology Sydney, Sydney, NSW, Australia
- h Sydney Institute of Marine Science, Mosman, NSW, Australia
- i CSIRO Environment, Hobart, Tasmania, Australia
- ^j Research School of Earth Sciences, Australian National University, Canberra, Australia
- k School of the Environment, The University of Queensland, Brisbane, Queensland, Australia
- ¹ Earth Sciences New Zealand, Wellington, New Zealand
- m Cooperative Institute for Research in Environmental Sciences, University of Colorado and NOAA Physical Sciences Laboratory, Boulder, CO, USA
- ⁿ Université de Toulouse, LEGOS (CNES/CNRS/IRD/UT3), Toulouse, France
- o Centre IRD de Nouméa, Nouméa, New Caledonia
- ^p National Oceanography Centre, Southampton, UK
- ^q Bureau of Meteorology, Melbourne, VIC, Australia

ARTICLE INFO

Keywords: Marine heatwaves Subsurface ocean dynamics Vertical structure Ocean extremes Biological impacts

ABSTRACT

Life is ubiquitous throughout the ocean, with species abundance and richness often greatest below the surface. As a result, ocean extremes throughout the water column may impact resident marine organisms and ecosystems. However, ocean extremes, such as marine heatwaves, have been commonly described based on surface observations. Given the importance of subsurface ocean processes, such as nutrient recycling, (de)oxygenation, and carbon transport, there has been an increasing focus on subsurface marine heatwaves (MHWs). Subsurface MHWs are prolonged warm ocean temperature extremes, and have a diversity of vertical structures linked with different driving mechanisms. Warming may be confined to the surface mixed layer; it may extend much deeper, potentially affecting the entire water column; it may appear only below the surface, with no surface signature, or it may be isolated near to or connected with the seafloor. Based on existing literature and a new analysis of subsurface MHW structure, we propose a comprehensive naming convention, differentiating between mixed layer, deep, thermocline, full depth, submerged and benthic marine heatwaves. Most surface-confined MHWs are associated with surface heat fluxes or shallow ocean advection or mixing. Conversely, many subsurface events are likely related to the vertical or horizontal displacement of temperature gradients/fronts, deep advection, and/or subduction of warm waters below the mixed layer. Different MHW vertical structures also have varying impacts on ocean biogeochemistry. However, due to the sparsity of physical, biogeochemical and biological observations, as well as the complexity of identifying and describing subsurface MHWs, there is limited understanding of the impact of subsurface MHW extremes. The nomenclature proposed in this paper seeks to provide a common language for understanding subsurface MHWs, thus enabling inter-disciplinary studies to quantify their impact.

^{*} Correspondence to: Climate Change Research Centre, Level 4, Mathews Building, The University of New South Wales, Sydney NSW 2052, Australia. E-mail address: n.malan@unsw.edu.au (N. Malan).

1. Introduction

Extreme temperatures associated with marine heatwaves (MHWs) are significant because of their impact on ecological systems globally, including in the coastal (Smith et al., 2024), pelagic (Brodeur et al., 2019b) and benthic (Amaya et al., 2023) realms. These impacts include microbial community changes (Brown et al., 2024), declines in biodiversity (Smale et al., 2019), loss of foundation species (Wernberg et al., 2013; Smith et al., 2024), and modified distributions of predators and prey (Gomes et al., 2024). Ecological impacts can occur at all trophic levels — from microbes to large marine predators, and from the individual through to the population level, as critical thermal thresholds are exceeded. Changes in one trophic level can have cascading implications for the whole ecosystem. As a result, MHWs can have enormous economic impacts with reported costs of individual MHW events exceeding US\$800 million in direct losses or US\$3.1 billion in indirect losses of ecosystem services for multiple years (Smith et al., 2021).

There are now many hundreds of studies that examine MHWs, including their definition, characteristics, proximate causes, links to remote drivers, predictability, species impacts, ecosystem impacts, fisheries impacts and associated socioeconomic consequences (e.g. Oliver et al., 2021; Smith et al., 2021; Capotondi et al., 2024). The majority of these studies have been focused on MHWs identified at the surface of the ocean, primarily because satellite observations of surface temperatures allow for high-frequency and high-resolution near-global real-time monitoring. However, temperature extremes also extend beyond the surface, and are not always visible in surface data (Sun et al., 2023). In some cases, surface signatures of MHWs can dissipate, whilst the subsurface MHW conditions persist even in the absence of the surface anomalies (Jackson et al., 2018). There are also ocean processes that can drive temperature extremes in the subsurface ocean without any surface expression (Gawarkiewicz et al., 2019; Schaeffer et al., 2023; Wyatt et al., 2023). These subsurface MHWs often have intensities that exceed those of surface events, especially around the thermocline depth (Schaeffer and Roughan, 2017; Hu et al., 2021).

With the majority of research focused on surface MHWs, it follows that our knowledge of their impacts is similarly biased to the surface. However, life inhabits all ocean depths. The greatest biomass and biodiversity occur on the continental shelves where ocean currents, strong mixing, upwelling and terrestrial inputs deliver the limiting nutrients that fuel primary productivity (Simpson and Sharples, 2012; Walsh, 2013), the basis for higher trophic levels. In the upper sunlit layers of the open ocean, the microscopic phytoplankton that underpin much of the marine food web (Fig. 1) are also affected by MHWs (Le Grix et al., 2021; Sen Gupta et al., 2020). In optimising for both light and nutrients, these primary producers can form chlorophyll-a maxima many tens of metres below the surface, in proximity to the reservoir of nutrients below the thermocline (Cullen, 2015; Silsbe and Malkin, 2016). Phytoplankton, whose distribution is predominantly determined by ocean currents and mixing (Purcell, 1977), are grazed by zooplankton that swim hundreds of metres through the water column as part of their daily vertical migration. Zooplankton are in turn consumed by higher trophic level predators that can actively dive thousands of metres (Hernández-León et al., 2020; Wirtz et al., 2022).

Important ecosystems also exist below the euphotic zone. On the continental shelf, as light diminishes with depth, diverse populations of vulnerable benthic species such as sponges (Perkins et al., 2022) and deep water corals are found on the seafloor. Further offshore, the open ocean's mesopelagic zone (200–4000 m), where light levels are too low for photosynthesis, is home to some of the most abundant organisms on earth, from viruses and protists, crustaceans, and deep dwelling fish such as anglerfish (Haddock and Choy, 2024), all the way through to deep diving megafauna such as sperm whales and elephant seals (Braun et al., 2022). Complex foodwebs and patterns can occur, such as subsurface maxima in abundance and species richness, with abundance

peaking as deep as 2000 m in the case of polychaetes, or 500 m in the case of fishes (Martini and Haddock, 2017; Haddock and Choy, 2024). MHWs are known to impact the predator–prey interactions at depth, with the vertical distribution of mesopelagic fishes deepening by up to 100 m during the 2015–16 MHW in the California Current (Iglesias et al., 2024).

The historical focus on surface MHW research (ignoring the subsurface) largely stems from the need for datasets with high frequency (e.g. daily, to resolve short-lived events) and long duration (to be able to define a baseline). In this regard, satellite temperature data have underpinned MHW research at the ocean surface, with gapfree optimally-interpolated products providing near global coverage of temperature at daily timescales and resolutions of 25 km or smaller since the early 1980s (e.g. Reynolds et al., 2002). Despite the recent increase in subsurface information observed by Argo profiling floats, and other observational platforms such as gliders and moorings, the subsurface ocean is comparatively very sparsely sampled, both in space and time. Past MHW studies using Argo data relied on satellite SST in order to first identify the presence of MHWs, and subsequently study their vertical structure (Elzahaby and Schaeffer, 2019; Scannell et al., 2020; Zhang et al., 2023). However, model reanalyses suggest that this approach neglects the 20%-40% of marine heatwaves that have no surface expression (Sun et al., 2023).

Data scarcity is even more problematic for the biological and biogeochemical (BGC) variables needed to understand the impact of MHWs on ocean chemistry and ecosystems. The only well-resolved (in space and time) near-global dataset that extends for multiple decades is satellite ocean colour, that is limited to estimating surface productivity. Although the number of Argo floats with biogeochemical sensors is rapidly growing, we are still far from reaching the float density required to resolve BGC variability in most regions of the ocean (Biogeochemical-Argo Planning Group, 2016). Additionally, Argo floats are restricted to operating in the deep ocean, and so cannot fill the data gap in shelf waters. Even with a large network, several decades of data would be required to form a biogeochemical baseline from which extremes can be identified. Ecological data in the subsurface, particularly in areas distant from the coast, rely on individual local or regional sampling programmes that target different species and collect different types of information. Due to this data sparsity and methodological diversity, it is challenging to apply these datasets to the systematic examination of subsurface MHWs and their impacts on marine life.

Surface MHW analysis is underpinned by a well-established theoretical framework centred around the mixed layer heat budget (Holbrook et al., 2019). Air–sea heat fluxes, together with ocean advection and mixing processes acting on the ocean mixed layer, explain the evolution of surface temperature and extremes. The local processes may in turn be modulated by large-scale modes of variability, e.g. El Nino - Southern Oscillation (Holbrook et al., 2019, 2021), Madden-Julian Oscillation (Manta et al., 2018; Salinger et al., 2020; Dutheil et al., 2024; Gregory et al., 2024), Pacific decadal variability (Capotondi et al., 2022; Ren et al., 2023), which may all be modified by anthropogenic climate change (Oliver et al., 2018; Holbrook et al., 2019).

In the deep ocean, however, away from the direct influence of the atmosphere, the drivers of temperature variability will often be different from the drivers of surface MHWs. Except for shortwave penetration in the photic zone, latent and sensible fluxes from ice shelves, and a few areas of hydrothermal activity, there are no subsurface sources or sinks of heat. Below the surface mixed layer, which is strongly coupled to the atmosphere, 'heave', the vertical movement of isopycnals (Hu et al., 2021) or anomalous advection and lateral movement of temperature fronts are likely to be major causes of extreme temperatures at given locations (Gawarkiewicz et al., 2019). Such dynamical processes involve redistribution, rather than changes in the total amount of heat. Likewise, in coastal systems, wind-driven downwelling can cause bottom-intensified MHWs by pushing isotherms down along the

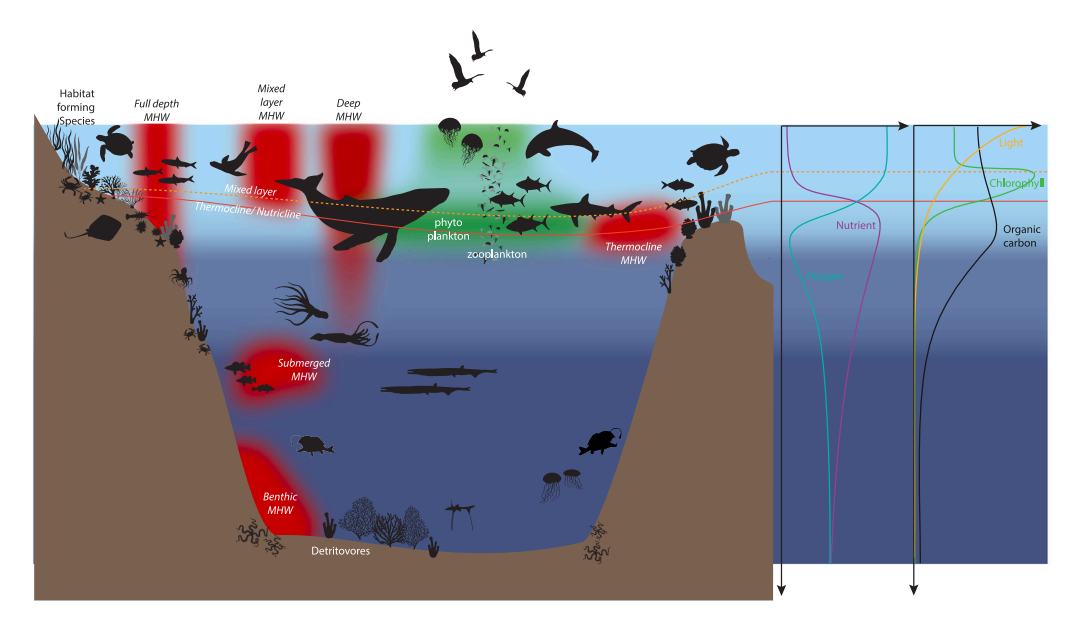


Fig. 1. A schematic view of the vertical distribution of life, biogeochemical properties, and six MHW vertical structures.

continental slope (Schaeffer et al., 2023). These redistributive driving mechanisms, heave and frontal movement, together with the characteristics of the local stratification, can give rise to a diversity of vertical temperature structures, and there have been recent efforts to classify sets of MHW types based on the location in the water column of the extreme temperatures (Schaeffer et al., 2023; Sun et al., 2023; Zhang et al., 2023). However, these studies used either a particular dataset or region, did not consider MHWs with no surface signature, or did not consider the evolution of MHW vertical structure over time, making them difficult to compare with each other, and apply to future studies.

The purpose of this work is fourfold. First, to advance the investigation and understanding of subsurface MHWs, we propose a more complete categorisation of subsurface MHW structures which extends the existing literature (Schaeffer et al., 2023; Sun et al., 2023; Zhang et al., 2023) through new analyses of the vertical structures of a large set of coastal and open ocean subsurface MHWs using different observational and model platforms. In doing so we adapt the classical Hobday et al. (2016) MHW definition to identify extreme profiles. Secondly, we discuss the possible physical drivers of each type of surface and subsurface MHW, providing case studies for many of these mechanisms. Thirdly, we consider the biogeochemical and ecological impacts of different types of vertical MHW structure. Finally, we discuss the limitations posed by the ocean observing technologies and datasets available today for identifying and studying each MHW type, and discuss future opportunities.

2. Methods

To examine and categorise subsurface temperature extremes, we use variations on an existing MHW definition (Hobday et al., 2016). We make use of daily climatologies from mooring and ocean model output, and monthly state estimates from a gridded Argo product. To consider the full range of MHW vertical structures and to highlight different driving mechanisms we present analysis and case studies using a variety of observational platforms in different regions, representing both the coastal and open ocean, as well as a global high-resolution ocean model output (see Fig. A.10 for a map showing the location of all sites considered in the analysis). These datasets offer different strengths and weaknesses. Details of these datasets are below, followed by the methodology used to identify extreme profiles. We note that there are a large range of methods available for estimating the mixed layer and thermocline depths, and endeavour, in each case, to choose the method most appropriate for each dataset, as detailed in the sections below.

2.1. Coastal mooring data

To assess subsurface MHWs at a single point in a region with a wide range of dynamic regimes, we use a decade of data (2010-05-31 to 2020-05-31) from the Australian Integrated Marine Observing System (IMOS) PH100 National Reference Station mooring located at 34.1 °S, 151.2 °E on the continental shelf to the east of Sydney, Australia (Roughan et al., 2022). At this location, the mooring experiences both wind and current-driven upwelling, as well as the strong frontal activity associated with the inshore edge of a Western Boundary Current. The mooring consists of a thermistor string at 8 m intervals from 15 m depth to the seafloor (100 m). As in situ surface values are not measured, estimated surface values are derived from daily satellite-measured SST data (see Roughan et al. (2022) for a detailed methodology). The temperature data are then interpolated onto a 1 m resolution vertical grid. As the mooring only measures salinity at the surface and bottom, we identify the base of the mixed layer as the depth where the linearly interpolated temperature first drops by 0.2 °C below the surface temperature (de Boyer Montégut et al., 2004). The thermocline is defined as where the vertical temperature gradient is at its maximum.

2.2. Ocean model output

Acknowledging the scarcity of appropriate subsurface observations and to provide a dynamically consistent global perspective, we use global 3d daily mean Conservative Temperature output for the period 1998 to 2018 from ACCESS-OM2-01, an eddy-permitting 1/10° resolution ocean and sea ice model driven by 3-hourly 0.5625° resolution air temperature, humidity, radiation, precipitation, runoff and wind fields from the JRA55-do v1.4.0 reanalysis (Tsujino et al., 2018). The configuration is based on Kiss et al. (2020), with updates described by Solodoch et al. (2022). The ocean z* vertical coordinate has 75 levels and resolution that coarsens smoothly from ~1.1 m at the surface to ~200 m at the maximum depth of ~5800 m. The model is initialised in 1958 from January climatological temperature and salinity from the World Ocean Atlas 2013 v2 (WOA13; Locarnini et al. (2013), Zweng et al. (2013)) and surface salinity is weakly restored to the WOA13 monthly climatology. The base of the mixed layer is identified using a density threshold of 0.03 kg.m-3 relative to the surface (de Boyer Montégut et al., 2004), and the thermocline is identified where the vertical temperature gradient is at its maximum after applying a 7 point Savitsky-Golay filter.

2.3. Gridded argo

Argo data have been used in multiple studies of subsurface signatures of surface MHWs. We use the Roemmich and Gilson (2009) gridded Argo data product to identify subsurface MHWs in an openocean MHW hotspot located at 40 °S-50 °S, 120 °W-140 °W in the Southern Ocean, a region of strong frontal activity (Sokolov and Rintoul, 2002) as well as Argo case study 1 and 2, in the tropical ocean. The gridded Argo dataset contains the monthly climatological mean fields of temperature and salinity from 2004-2018 and their monthly anomaly fields for each year since 2004. The data are provided on a 1°-by-1° spatial grid, with 58 pressure levels from 2.5 to 2000 dbar. A seasonally-varying monthly MHW threshold calculated from this dataset is used in Figs. 3 (c) and 8 (b-c). A non-seasonally varying monthly percentile threshold is used in Fig. 9 (d & f). Both approaches have previously been used in the literature (Frölicher et al., 2018; Jacox et al., 2020; Capotondi et al., 2022). For a discussion around departures from the formal MHW definition necessary for different datasets, please see the section below on data challenges. We identify the base of the mixed layer following a fixed temperature threshold approach (de Boyer Montégut et al., 2004), with a threshold of 0.2 °C. The thermocline is again identified where the vertical temperature gradient is at its maximum.

2.4. Satellite altimetry

Geostrophic velocities for mooring case study 1 were obtained from an OceanCurrent product distributed by IMOS that merges satellite altimetry with sea level elevation measurements from coastal tide gauges (Deng et al., 2011) to improve accuracy in coastal regions.

Sea level for case study 2 was obtained from the Copernicus Climate Change Service (C3S), 2021 DT merged two-satellite Global Ocean L4 Monthly Means of Sea Level Anomalies and Derived Eddy Kinetic Energy, Version vDec2021.

2.5. Sea surface temperature

Sea surface temperatures for mooring case study 2 were obtained from the IMOS day and night-time L3S product derived from the AVHRR instruments on NOAA polar orbiting satellites (Griffin et al., 2017). The SST data are daily, cover the period 1992–present and have a spatial resolution of 0.02° in a domain 70 °E to 170 °W, 20 °N to 70 °S.

2.6. The marine heatwave severity index

To compare the strength of MHWs across regions, depths and datasets we use the MHW severity index (from here on referred to as severity), following Sen Gupta et al. (2020), defined as:

$$S_{z,t} = \frac{T_{z,t} - T_{z,d}^{clim}}{T_{z,d}^{PC90} - T_{z,d}^{clim}} \tag{1}$$

where, at a given location $T_{z,d}^{clim}$ is the daily-varying climatological mean of temperature $T_{z,d}$ at each depth in the dataset and $T_{z,d}^{PC90}$ is the daily-varying climatological 90th percentile of temperature at each depth in the dataset. An 11-day moving and 31-day smoothing window is applied when calculating the climatologies (with the exception of the monthly Argo product, where no smoothing is applied). The severity index is a continuous extension of the Hobday et al. (2018) MHW categorisation scheme. It employs temperature anomalies normalised by the difference between the mean and 90th percentile climatologies. Severity exceeding 1, 2, or 3 corresponds to moderate, strong or extreme category events, respectively (Hobday et al., 2018). This normalisation is especially important when comparing temperature extremes across different depths, as some parts of the water column,

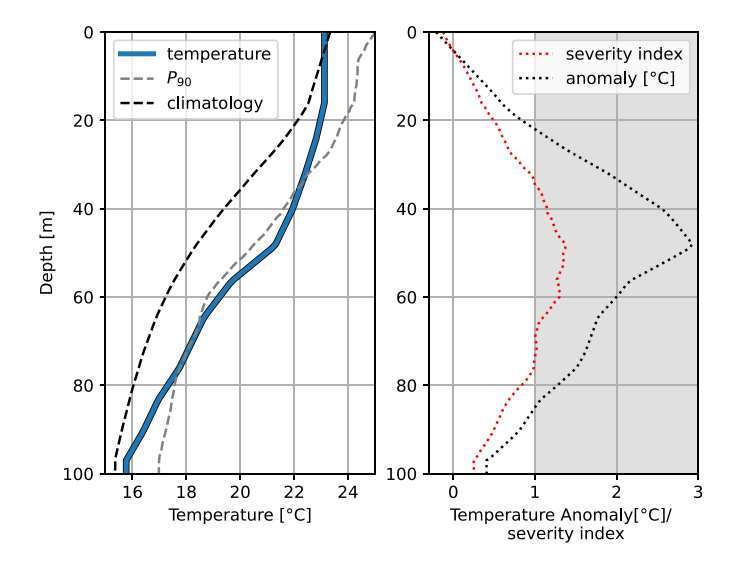


Fig. 2. An example profile showing (a) a daily temperature profile (taken from the PH100 mooring) compared to its corresponding daily climatological mean and 90th percentile profiles, as well as (b) the associated anomaly (from the mean climatology) and marine heatwave severity index. The grey shading shows the severities that would meet the MHW condition. In this case a MHW is present between about 35 and 70 m.

such as the thermocline, will have much higher temperature variability than others. Use of the severity index, as opposed to discrete categories, quantifies the relative intensity of marine heatwaves within the water column, enabling comparison across depths and revealing the vertical coherence and structure of the MHW. Fig. 2 shows an example of how the temperature profile, mean and 90th percentile climatologies, temperature anomaly, and severity index relate through the water column. This effect can also be explored by examining the difference between maximum severity and intensity in Table A.1. Given that marine organisms are adapted to ambient levels of variability in their environment, severity likely represents a more biologically meaningful metric of thermal stress than temperature anomaly.

2.7. Identification of extreme profiles

We identify extreme temperature profiles as those with MHW severities that exceed 1 (i.e. > than the MHW threshold) at one or more depths within the profile. For the mooring and the ocean model output this is based on a daily varying 90th percentile climatology, while for Argo, monthly climatologies are used.

2.8. Surface heat flux and ekman pumping

Four observational case studies below demonstrate drivers of different MHW types.

Daily heat flux components and 10 m wind from the ERA5 reanalysis (Hersbach et al., 2020) are used. Total surface heat flux is calculated as:

$$Q_{net} = SW_{net} + LW_{net} + SHF + LHF \tag{2}$$

where Q_{net} is the net surface heat flux, SW_{net} is the net shortwave radiation, LW_{net} is net longwave radiation, SHF is the net sensible heat flux and LHF is the net latent heat flux.

Ekman pumping anomalies are used to estimate the vertical movement of the thermocline due to local winds and are calculated as:

$$w_E = \nabla \times (\frac{\tau}{\rho f}) \tag{3}$$

where τ is the surface wind stress, ρ is the nominal density of seawater (1025 kg m³) and f is the Coriolis parameter.

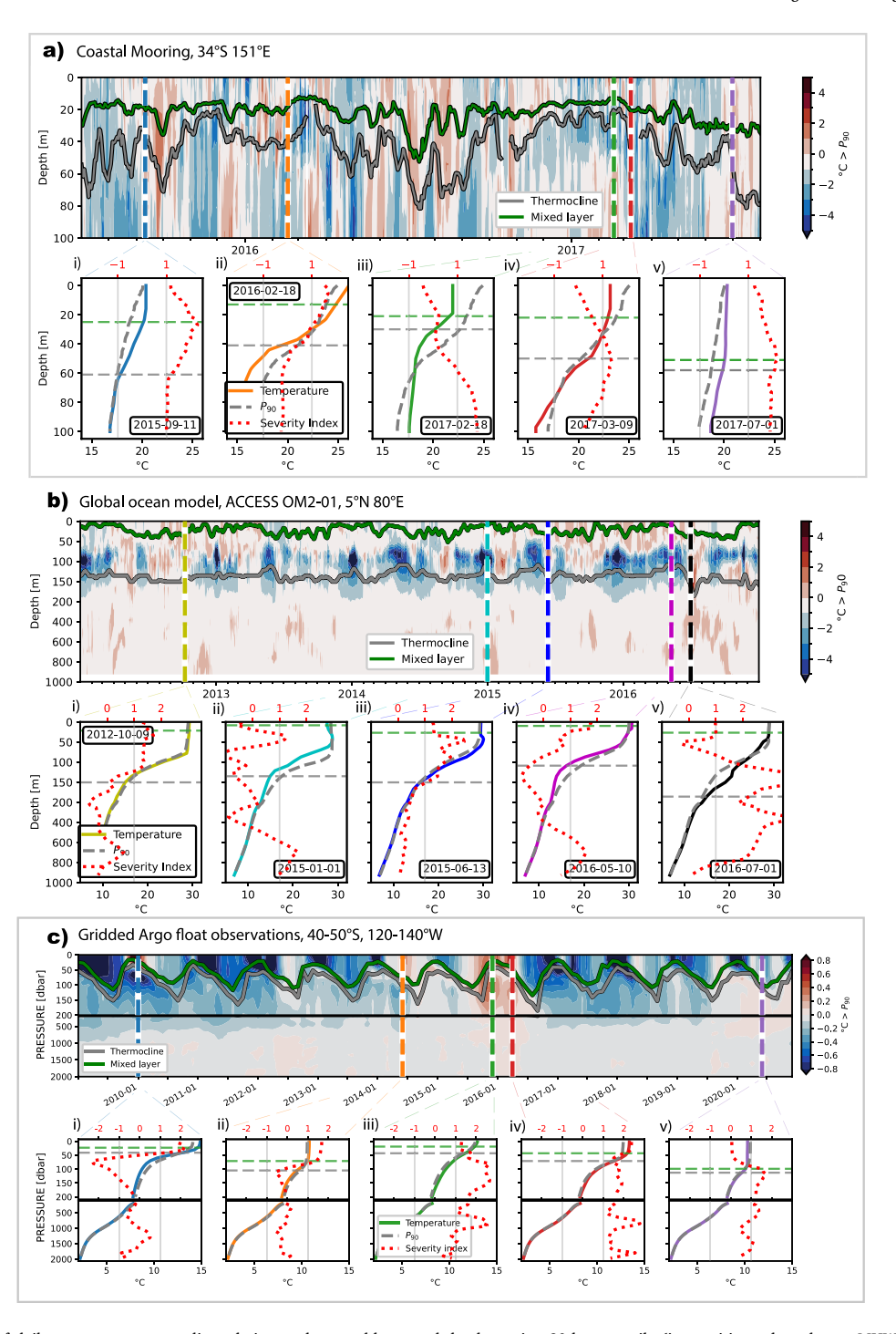


Fig. 3. Depth-time series of daily temperature anomalies relative to the monthly — and depth-varying 90th percentile (i.e. positive values denote MHW conditions) from (a) the coastal mooring site at 34 °S off eastern Australia, (b) ACCESS-OM2-01 at 5 °N, 80 °E in the tropical Indian Ocean and c) monthly gridded Argo at 40 °S-50 °S, 120 °W-140 °W in the Southern Ocean. Panels i–v for each dataset show absolute temperature profiles (coloured lines), climatological 90th percentile (P90) and severity index for five marine heatwave events with distinct vertical structures, corresponding to dates indicated by the colour coded vertical lines in panels a, b and c. The green and grey dashed lines represent the mixed layer and thermocline, respectively, on that particular day.

3. Heatwave typology

Depth-time analysis of temperature anomalies relative to the local 90th percentile MHW threshold from daily coastal ocean moorings (Fig. 3a), ACCESS-OM2-01 (Fig. 3b) and monthly gridded Argo data (Fig. 3c) show the evolution of extreme temperatures over time. Clearly there are large differences in vertical scales between the coastal and open ocean (100 m vs >1000 m), as well as substantial excursions of the mixed layer and thermocline depth across time. We highlight a subset

of times when MHWs occurred (lower panels of Fig. 3 a, b and c). By examining where temperatures (solid lines) exceed the MHW threshold (grey dashed lines), or equivalently where severity (red dotted line) exceeds 1 on Fig. 3, we can see that the MHWs are detected in different parts of the water column. For example during February 2017, the coastal mooring site (Fig. 3a(iii)) shows temperatures well over the MHW threshold in the lower half of the water column at this location (60–100 m depth), while temperatures in the upper half of the water column are below the threshold. All three time series (Fig. 3 a, b and c)

Table 1
Characteristics of existing subsurface marine heatwave typologies.

Data source	Data type	Region	Depth range	No surface expression	Proposed MHW types
Schaeffer et al. (2023)	Mooring	Coastal regional	0–65 m	Yes	Shallow, Subsurface, Extended
Sun et al. (2023)	Model Reanalyses	Global	0-200 m	Yes	Subsurface, Mixed
Zhang et al. (2023)	Argo	Global	0–1000 m	No	Shallow, Deep, Subsurface- intensified, Subsurface-reversed

also show examples where MHW severity is highest in the mixed layer (Fig. 3a(ii), 3b(iv), 3c(i)).

Various studies have proposed MHW classifications based on their vertical structure using mooring data, Argo profiles or model reanalysis, summarised in Table 1. Schaeffer et al. (2023) analysed a long-term mooring record in 65 m of water at a coastal site and proposed 3 types of marine heatwave: (i) 'shallow marine heatwaves' extend from the surface through the mixed layer but then decay rapidly, (ii) 'subsurface marine heatwaves', form exclusively below the mixed layer and (iii) 'extended marine heatwaves', where extreme temperatures exist throughout the water column. Zhang et al. (2023) combined Argo and satellite measurements to identify the subsurface expression for 4 types of surface marine heatwaves including: (i) 'shallow', defined as within the mixed layer, (ii) 'deep', extending deeper than the mixed layer, (iii) 'subsurface reversed', where there are warm anomalies at the surface, but cool anomalies at the thermocline and (iv) 'subsurface intensified', where anomalies are largest at the thermocline. Using ocean reanalyses, Sun et al. (2023) employed a 3-D spatiotemporal tracking scheme to divide large marine heatwave events into (i) 'surface' (has a continuous surface signal over the duration of the event), (ii) 'subsurface' (has no surface signal) and (iii) 'mixed' (has a surface signal, but not throughout the lifespan of the MHW) events.

These classifications of subsurface MHWs vary somewhat as they span both global open ocean and regional shelf studies, and employ datasets based on different temperature sensing platforms. A difficulty that arises is how to compare the vertical structure of MHWs at different locations over vastly different water depths, across different times of the year and using varied data sources. All of the above studies highlight the importance of the mixed layer, which denotes the extent of surface confined MHWs, and of the thermocline, where small vertical displacements of sharp temperature gradients can cause large variations in temperature. However, the variation in mixed layer and thermocline depths over the course of the annual cycle or at different locations (Fig. 3) means that systematically identifying MHW types across space and time is challenging. For example, Zhang et al. (2023) acknowledge this challenge and use a temporally and spatially varying mixed layer depth in their classification, but restrict the mixed layer to being shallower than 100 m, as well as aggregating profiles spatially in 2° × 2° bins and temporally over the course of each surface-identified MHW. This approach makes some account for a variable mixed layer depth, but does not allow for MHW vertical distribution to change over the course of the MHW life cycle, for example from a surface type to a subsurface type, a behaviour which has been well-documented (Jackson et al., 2018; Köhn et al., 2024) in previous studies, particularly for longlasting events. Additionally, when computing the mean profiles of MHW types, averaging together profiles of varying mixed layer depths obscures whether or not the anomaly has occurred within the mixed layer or below.

To classify the vertical structure of MHWs using physical ocean features (rather than absolute depth) as the vertical coordinate, we consider the surface, mixed layer depth, thermocline depth and ocean floor (or maximum depth extent of the data) as the reference levels for the water column. These reference levels separate the 3 fundamental layers of the global ocean: the mixed layer, where tracers (like heat,

salt, carbon and oxygen) are exchanged with the atmosphere and properties are relatively homogeneous with depth; the thermocline, where stratification is typically strongest; and the deep ocean where temperature is relatively constant over time and depth (Sallée et al., 2021; Romero et al., 2023). The mixed layer and the thermocline also play a key role in biological and biogeochemical activities. Indeed, phytoplankton is rapidly redistributed within the mixed layer, while the thermocline is approximately co-located with the nutricline. Physically, using the mixed layer and thermocline depths as reference levels simplifies the study of what causes MHWs at different depths, as different driving mechanisms typically act predominantly within the mixed layer, at the thermocline or at greater depth. For example, heat entering the ocean surface is quickly redistributed through the mixed layer via strong turbulent mixing processes, and vertical displacements of the water column associated with Ekman pumping or the passage of planetary waves can result in large temperature variations within the thermocline. Thus, although the mixed layer and thermocline may be close to each other in physical space, they represent different dynamical and biological regimes and therefore are separated in our analysis.

Can we quantify the common vertical structures of MHWs using this new vertical frame of reference? In order to appropriately compare MHWs in difference seasons and locations, as detailed above, we apply a linear rescaling of the depth coordinate such that temperatures at the surface, mixed layer, thermocline and lowest level are remapped to 0, $\frac{1}{3}$, $\frac{2}{3}$ and 1 of the water column respectively and temperatures at intervening depths are linearly interpolated.

To separate out the common vertical structures we apply a clustering algorithm to scaled profiles from both the open ocean (using output from a global ocean model) and a coastal site (the PH100 mooring). For the open ocean we apply the agglomerative clustering algorithm (Pedregosa et al. (2011): see Appendix and Fig. B.11 for the detailed profile selection, rescaling and clustering methodology) to $> 30\,000$ vertically rescaled profiles of MHW severity index (to a maximum depth of 1500 m) extracted at daily resolution from 100 randomly selected locations in a global eddy resolving ocean model (ACCESS-OM2-01, Fig. 4f) between 60 °N and 60 °S. All profiles are selected so that they contain an extreme temperature at one or more depths (for the global analysis severity > 2 is used). In both cases, the number of clusters is chosen using the dendrogram of clusters, and then refined to a level where clusters show distinct vertical structures, rather than varying strengths of the same vertical structure.

The global analysis of ACCESS-OM2-01 temperature profiles (Fig. 4) includes profiles from a wide range of different oceanic regimes. Dividing into 5 clusters (note that clusters containing less than 300 profiles are removed from the analysis) gives 5 distinct patterns of vertical MHW structure. Examining the mean of all profiles making up the first cluster (Fig. 4a), we find the largest MHW severity in the mixed layer, quickly dropping off below and with no elevated anomalies at the depth of the thermocline. In the second (Fig. 4b), MHW severity is still elevated in the mixed layer, and high severities extend to the depth of the thermocline. The third cluster (Fig. 4c) shows highest severities concentrated near the thermocline with no surface signature. In contrast, the fourth cluster (Fig. 4d) exhibits MHW conditions throughout the water column. The final cluster (Fig. 4e) only exhibits high severity below the thermocline.

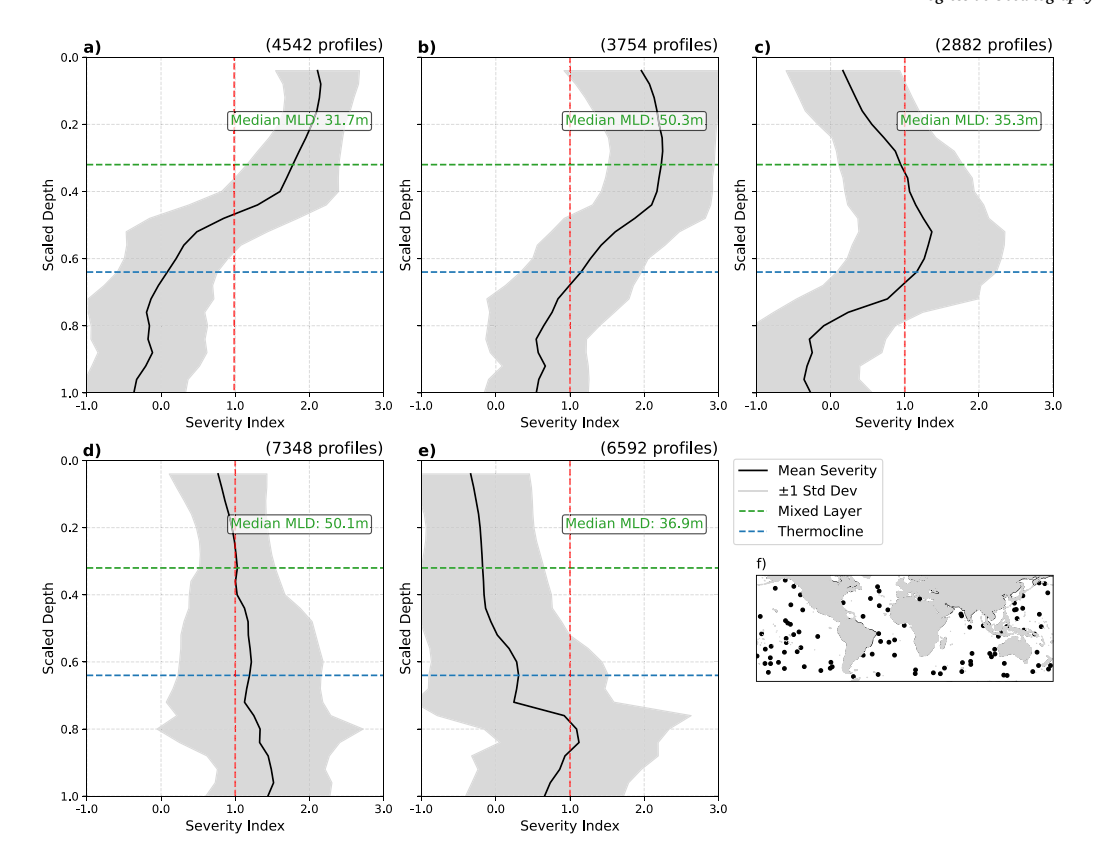


Fig. 4. Global clustering of MHW severity index profiles, containing MHW severity> 2 at a minimum of one depth (panels a—e) from 100 random locations (panel f) in ACCESS-OM2-01. The black profiles represent the mean of each cluster, shaded with one standard deviation. 'Scaled Depth' represents the water column scaled by the mixed layer (green dashed line) and thermocline depths (blue dashed lines). Severity index values greater than 1 (red dashed line) indicate MHW conditions. See Table A.1 for statistics.

To test whether these categories also appear in a dynamically complex coastal environment, we apply the same clustering methodology to >4000 daily profiles at a single location (Fig. 5f), the coastal PH100 mooring in 100 m water depth inshore of a western boundary current. Here due to the smaller sample size we use a lower threshold (i.e. severity >1) to detect a sufficient number of profiles for effective clustering.

We find important commonalities with the global analysis. The first cluster (Fig. 5a) exhibits highest severity near the surface although severity drops off towards the base of the mixed layer. In the second cluster (Fig. 5b), severity is uniform within the mixed layer, remaining elevated but tailing off towards the thermocline. The third cluster shows a peak in severity close to the thermocline, with no signature at the surface (Fig. 5c), while in the fourth cluster (Fig. 5d) the MHW severity threshold is exceeded throughout most of the water column. In the final cluster, severity peaks at the bottom, with no surface expression (Fig. 5e).

Whilst there are similarities between the clustering at the global and local scale, there are also differences. For example, in the global analysis (Fig. 4e), the fifth cluster represents MHWs below the thermocline and the bottom of the dataset, while in the coastal mooring clusters, the fifth cluster MHWs intensify towards the ocean floor (Fig. 5e). There is also a data limitation in the mixed layer at the coastal site due to the lack of temperature data between the surface and 15 m depth at PH100. Under most conditions this does not affect the analysis (the mean mixed layer depth is 23 m, but very surface intensified MHWs (Fig. 5a) are often associated with anomalously shallow mixed layers, not resolved by the mooring dataset as can be seen in linear drop off in severity from the surface to mixed layer in Fig. 5a. Thus some allowances must be made due to the differences between the global model, and coastal mooring datasets. However, the vertical structures in the cluster analyses lend themselves to very similar descriptions,

providing a common language which simplifies the description of MHW vertical structures globally.

Therefore, based on the categories proposed by Schaeffer et al. (2023), Zhang et al. (2023) and Sun et al. (2023), and informed by our analysis of observational and modelled datasets, merging together the common vertical structures from both the global open ocean and a coastal dataset, we propose a typology consisting of 6 primary types of marine heatwave vertical structures (Fig. 6):

Mixed layer MHW

Temperatures exceed the MHW threshold through the mixed layer, before dropping off below the base of the mixed layer (Fig. 6a). For example, Fig. 3a (ii) and Fig. 3c (i). This is analogous to the shallow MHW type discussed in Schaeffer et al. (2023) and Zhang et al. (2023). Interestingly, our global analysis shows that the average MLD for this category is the shallowest over all clusters (Fig. 4, Table A.1). This is consistent with enhanced warming when the mixed layer is shallow, such as in the summer, with surface heat fluxes acting on a reduced water volume.

Deep MHW

A MHW event with a surface expression where temperatures above the MHW threshold extend well below the mixed layer into the thermocline (Fig. 6b). For example, Fig. 3a (i), Fig. 3b (i), Fig. 3c (ii). Such MHWs have been discussed in the northeast Pacific during the Blob (Scannell et al., 2020), and in the Mediterranean Sea (Juza et al., 2022) often in the decaying stage of an MHW, and are analogous to Zhang et al. (2023)'s 'Deep MHW'. Although the global clustering shows mixed layer and deep MHWs to be similar in surface expression and structure, in our global cluster analysis they are associated with median mixed layers that are 60% deeper than mixed layer MHWs (Fig. 4 a,b).

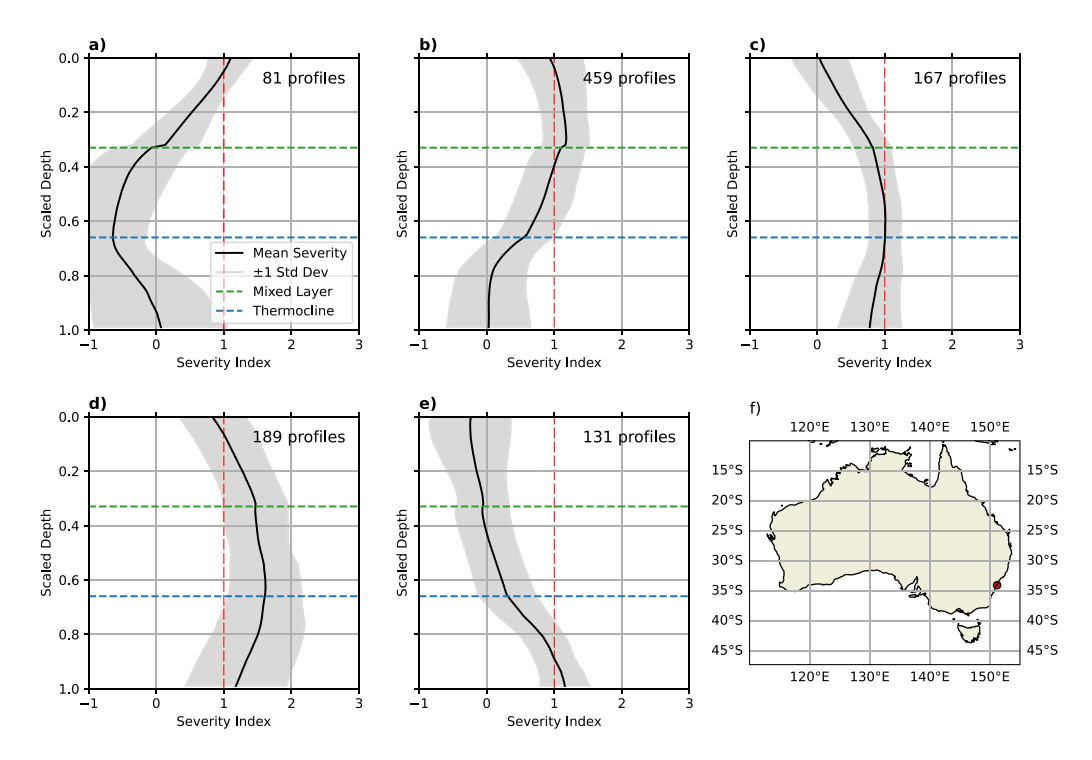


Fig. 5. Local clustering of MHW severity index profiles, containing MHW severity> 1 (panels a—e) from a decade-long coastal mooring time series (PH100, red dot in panel f). The black profiles represent the mean of each cluster, shaded with one standard deviation. 'Scaled Depth' represents the water column scaled by the mixed layer (green dashed line) and thermocline depths (blue dashed line), the red vertical dashed line represents the MHW threshold.

Thermocline MHW

A MHW event which has maximum severity near the thermocline, with minimal surface expression (Fig. 6c). For example, Fig. 3a (iv), Fig. 3b (v), Fig. 3c (v). These are analogous to Zhang et al. (2023)'s 'subsurface-intensified' MHW and have been observed by Wyatt et al. (2023) in the tropical Pacific and are typically associated with the vertical movement of the thermocline.

Full depth MHW

Temperature exceeds the MHW threshold through the entire water column; or at least across the vertical extent of the dataset (Fig. 6d). As such, it has a surface expression. For many real-world cases we can infer an impact on the full water column in shallow regions where we have observations that extend throughout the water column (e.g., Schaeffer et al. (2023), our Fig. 3a (v)). However, in the open ocean there are examples of continuous MHW conditions extending thousands of metres into the water column, e.g. Fig. 3c (iv)

Submerged MHW

Temperature exceeds the MHW threshold predominantly below the base of the thermocline, with no surface expression (Fig. 6e), and with no evidence of reaching the ocean floor. Extreme temperatures which occur in the relatively stable temperatures of the deep ocean, for example, Fig. 3b (ii).

Benthic MHW

A MHW event with maximum intensity at the ocean floor, with no surface expression (Fig. 6f). For example, Fig. 3a (iii). The identification of these events requires full depth information and are thus likely to

be most commonly identified on continental shelves. MHWs focused on the ocean floor with no surface expression have been identified around North America (Amaya et al., 2023; Großelindemann et al., 2022), also analogous to some observed examples of Schaeffer et al. (2023)'s 'subsurface' marine heat wave.

MHW events will often not fall cleanly into a single category. For example, we find heatwaves that have extreme temperatures through the mixed layer but with a maximum at the thermocline (Fig. 3b (iii)), indicating a combined thermocline/mixed layer MHW. Mixed layer MHWs also co-occur with submerged MHWs (Fig. 3b (iv), Fig. 3c (i)). Close to the coast, during times of deep mixing, mixed layers may extend to the sea floor. As such, there would be no distinction between surface and full depth MHWs. There are also many instances where we see the evolution from one type of MHW to another. For example, heat associated with a mixed layer MHW can mix downwards over time forming a deep MHW and then cool at the surface to become a thermocline MHW (as in Fig. 3b (iii)). The evolution of MHWs extending into the subsurface has been examined in detail in the northern and tropical Pacific in a regional ocean model (Köhn et al., 2024). They found one third of surface-identified MHWs extend below the mixed layer (deep MHWs by our classification) and that 24% of these propagate downwards, 20% propagate upwards, and less than half remain in contact with the surface over the course of their lifespans (thus transitioning from surface to thermocline MHWs by our classification). Thus, we have structured this typology to enable the type of marine heatwave to be described at each point in time, to capture the evolution of vertical structure. If the vertical structure of a MHW is defined as the mean structure of the event, this important evolution will not be resolved.

4. Drivers of different marine heatwave types

The processes driving surface MHWs have been widely studied, typically in the context of a mixed layer heat budget (Holbrook et al.,

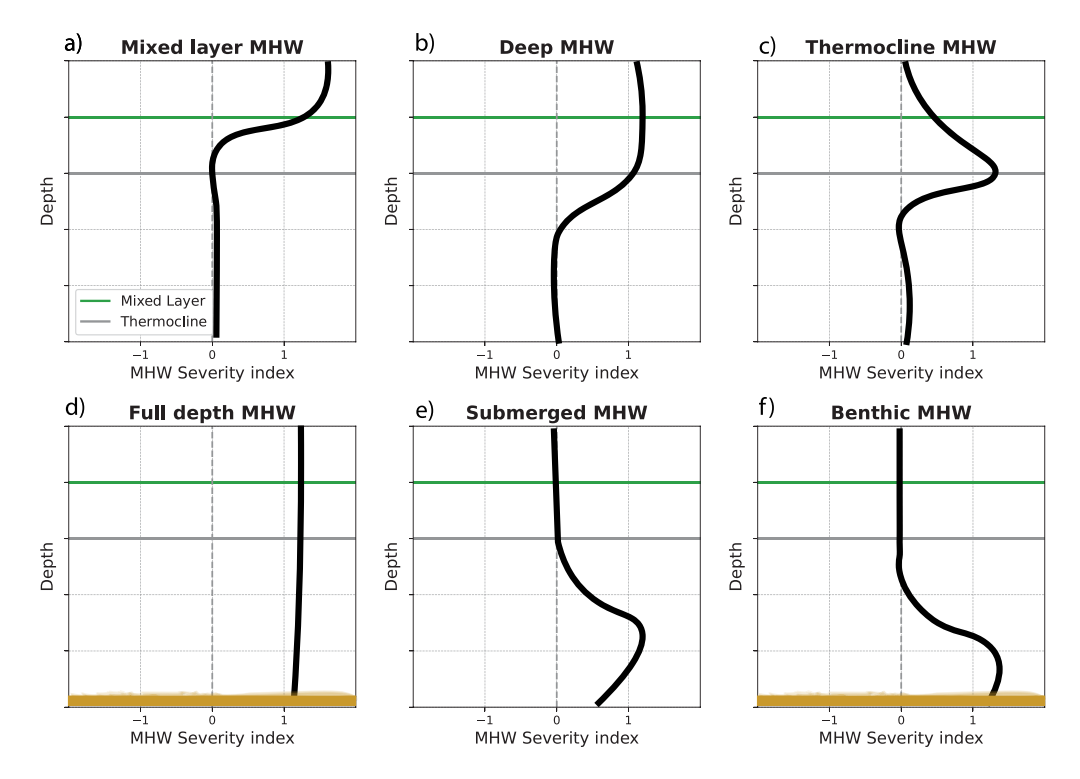


Fig. 6. Schematic representation of the 6 MHW types in relation to the base of the mixed layer and thermocline. Note that a severity index > 1 denotes marine heatwave conditions. Green and dark grey lines indicate the mixed layer and thermocline depths, respectively.

2019). In the mixed layer heat budget, the evolution of temperature averaged over the mixed layer depends on radiative and turbulent heat fluxes from the atmosphere, less any penetration of solar radiation out of the bottom of the mixed layer, together with ocean advective heat fluxes and horizontal and vertical mixing processes. Temperature variations are also strongly affected by the depth of the mixed layer and the volume of water being heated (Elzahaby et al., 2022). When identified by their surface expression, the largest events (Sen Gupta et al., 2020) have been most commonly associated with anomalously weak winds that lead to reduced evaporative cooling and weaker vertical mixing. However, in the subsurface ocean, there are typically no internal sources of heat (except in hydrothermal regions), and the role of ocean dynamics in creating temperature extremes by redistributing heat becomes more important (e.g. Großelindemann et al. (2022)). Global studies diagnosing the relative roles of atmospheric and oceanic processes in driving upper ocean MHWs report varying results based on their choice of depth range, e.g. the upper 10 m (Vogt et al., 2022), the upper 50 m (Bian et al., 2023) or the climatological mixed layer (Marin et al., 2022). Studies using a larger depth range report greater oceanic contributions and vice-versa. Use of the typology proposed here will remove this ambiguity and allow more precise attribution of the drivers of different MHW types.

A number of distinct mechanisms can drive the formation of MHWs, associated with the different subsurface MHW structure. Broadly, these mechanisms can be divided into: anomalous advection, frontal movement, vertical heave and surface heating. Most MHW types can be driven by one or more of these mechanisms, as detailed below.

Mixed layer MHW

Heat entering the ocean surface via air–sea fluxes or shallow surface currents (Fig. 7a) is quickly distributed through the well mixed surface layer. The depth of mixed layer MHWs typically extends a few 10 s of metres into the ocean although the depth and intensity may evolve

as the mixed layer deepens or shoals. These MHWs are typically associated with low wind speeds, anomalous air-sea fluxes (particularly reduced latent heat loss (turbulent) and/or enhanced solar (increased penetrative downward shortwave radiation) into the ocean, shallow warm advection and suppressed mixing at the base of the mixed layer (Fig. 7j). Mixed layer MHWs may also be related to preconditioning by an anomalously shallow mixed layer (Lee et al., 2023) that can give rise to enhanced surface warming during seasons of climatological temperature increase (i.e. during spring and summer), even without anomalously large surface heat fluxes (Fig. 7n). Many of the most iconic large scale MHWs are likely to have been mixed layer MHWs (at least in their initial phases), e.g. the Blob (Bond et al., 2015), the Blob 2.0 (Amaya et al., 2020)/18 Tasman Sea (Perkins-Kirkpatrick et al., 2019), the 2013/14 southwest Atlantic MHW (Rodrigues et al., 2019), the 2009/10 South Pacific event (Lee et al., 2010) and the 2012 Northwest Atlantic MHW (Chen et al., 2015).

Deep MHW

Such events may result from processes including advection by deep reaching currents (Fig. 7b) e.g. the 2015/16 Tasman Sea MHW (Oliver et al., 2017), deep mixing followed by re-stratification (Jackson et al., 2018), or the lateral movement of fronts or eddies with strong lateral temperature gradients that extend deep below the mixed layer (Fig. 7f). Mixed layer MHWs driven by surface fluxes can also transition into a Deep phase before being eroded at the surface to become a thermocline MHW (Fig. 7o, Scannell et al. (2020)).

Full depth MHW

These events will predominantly affect shelf regions, or areas of strong temperature fronts such as boundary currents. Such events may be related to the increased poleward penetration (Fig. 7c) or onshore intrusion of deep warm currents (Fig. 7 g) or eddies (Schaeffer et al., 2023; Wyatt et al., 2023). An example can be seen in the coastal PH100

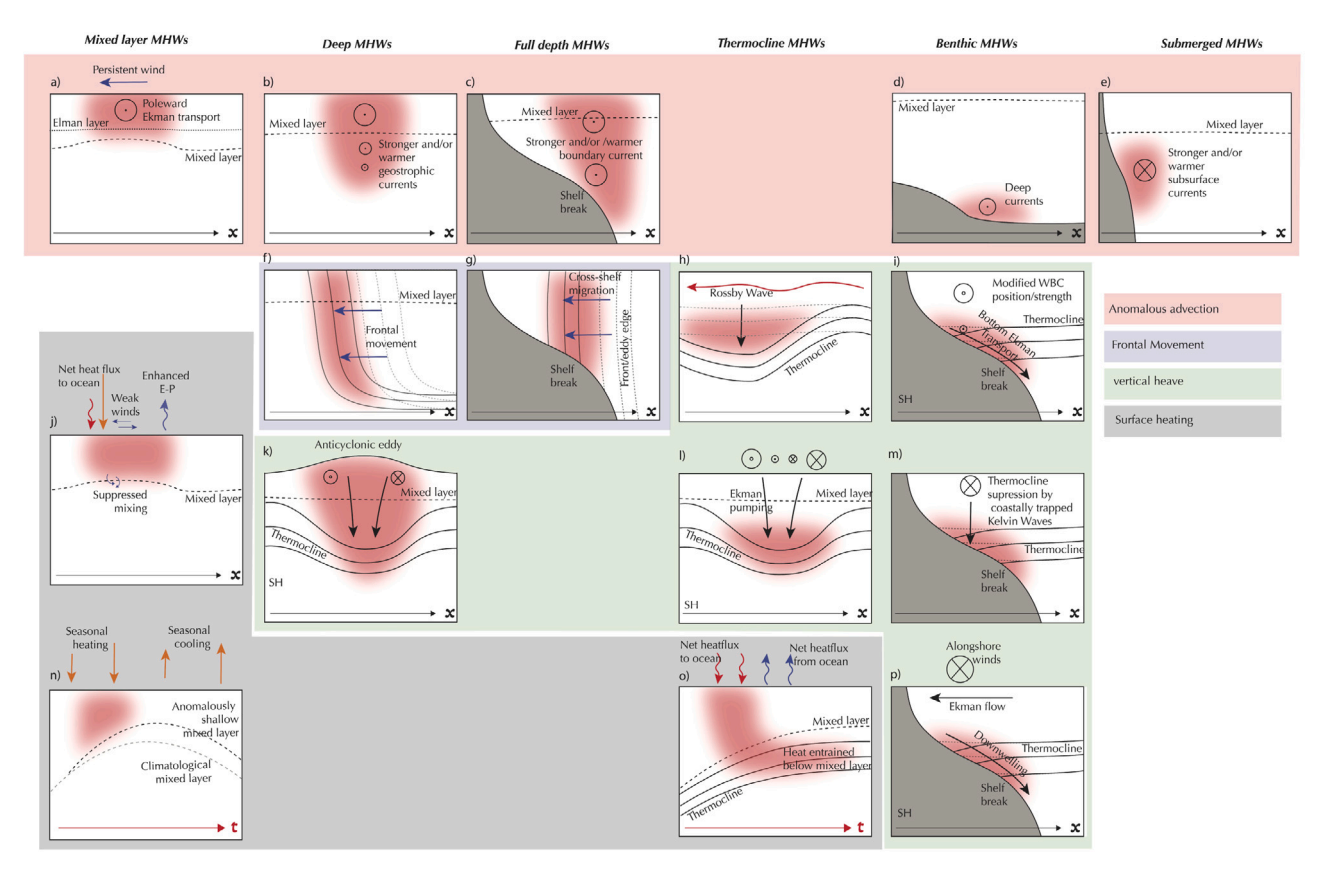


Fig. 7. Schematic of important driving mechanisms of each of the 6 types of subsurface marine heatwaves (columns). The shaded colours represent the four main sources of extreme warm temperatures: Anomalous advection, Frontal movement, vertical heave and surface heating. Note that panels showing oceanic drivers have space (x) on the x axis, while panels showing atmospheric drivers have time (x) on the x axis.

mooring data inshore of the East Australian Current, where the inshore edge of the western boundary current jet encroaches onto the shelf (Fig. 8 b-f).

Thermocline MHW

Many such events are associated with the vertical movement of vertical temperature gradients in the thermocline (a process known as heave). Downward heave, leads to an adiabatic warming at constant depth levels that is greatest at the thermocline (Fig. 71). Downward heave can result from coastal wind driven downwelling (Schaeffer et al., 2023), open ocean Ekman pumping (Hu et al., 2021), the passage of downwelling favourable Kelvin waves along the equator or along coastlines (Ryan et al., 2021), or Rossby waves in the interior ocean (Holbrook et al., 2011; Li et al., 2020) (Fig. 7h). Thermocline MHWs have also been found in the Tasman Sea (Elzahaby and Schaeffer, 2019), associated with the intrusion of heat at the edge of a large anticyclonic eddy, with the occurrence of thermocline MHWs concurrent with anticyclonic eddy activity also being observed globally from mooring observations (He et al., 2024).

Submerged MHW

In the deep ocean, temperature variability is small, and sources of anomalous heat are limited as there are no surface fluxes or vigorous circulation as seen in the surface layers. Due to the lack of appropriate observations, our knowledge of high frequency temperature variability below the thermocline is limited. However, several subsurface mechanisms could still potentially drive submerged MHWs. In equatorial regions, for example, changes in the strength of deep equatorial jets (Ménesguen et al., 2019) or the deep western boundary currents (Meinen et al., 2013) can change the advection of heat well below the thermocline (Fig. 7e).

Benthic MHW

On the continental shelf, benthic MHWs have been linked to down-welling/suppressed upwelling (Fig. 7p), due to changes in alongshore winds in summer when the water column is stratified (Schaeffer et al., 2023). On the west coast of North America, it has been suggested that benthic MHWs could be associated with El Nino events, due to the passage of downwelling coastally trapped waves (Fig. 7m, Amaya et al. (2023)). Benthic MHWs have also been associated with bottom intrusions of warm water along shelf break fronts (Großelindemann et al., 2022).

Below we highlight a number of case studies of MHWs associated with distinct driving mechanisms:

4.1. Mooring case study 1 and 2 - Coastal MHWs on the southeast Australian shelf

We compare two different types of MHWs at the mooring PH100 on the shelf inshore of the East Australian Current (EAC), each with a distinct driving mechanism. On the 18th of February 2016, there was a strong heat flux anomaly into the ocean (Fig. 8a). Associated with this, temperatures in the upper 40 m of the water column (the mixed layer) exceeded the MHW threshold for more than 5 days (Fig. 8b), resulting in a mixed layer MHW. A different dynamic occurred during June of the following year, when a full depth marine heatwave formed. This occurred when the warm poleward-flowing EAC jet moved from its normal position (Fig. 8c) to encroach onto the shelf (Fig. 8e). The resulting frontal movement caused temperatures through the full water column to warm from a normal state, with slight warm anomalies near the bottom (Fig. 8d), to exceeding the 90th percentile threshold at all depths, resulting in a full depth MHW (Fig. 8f).

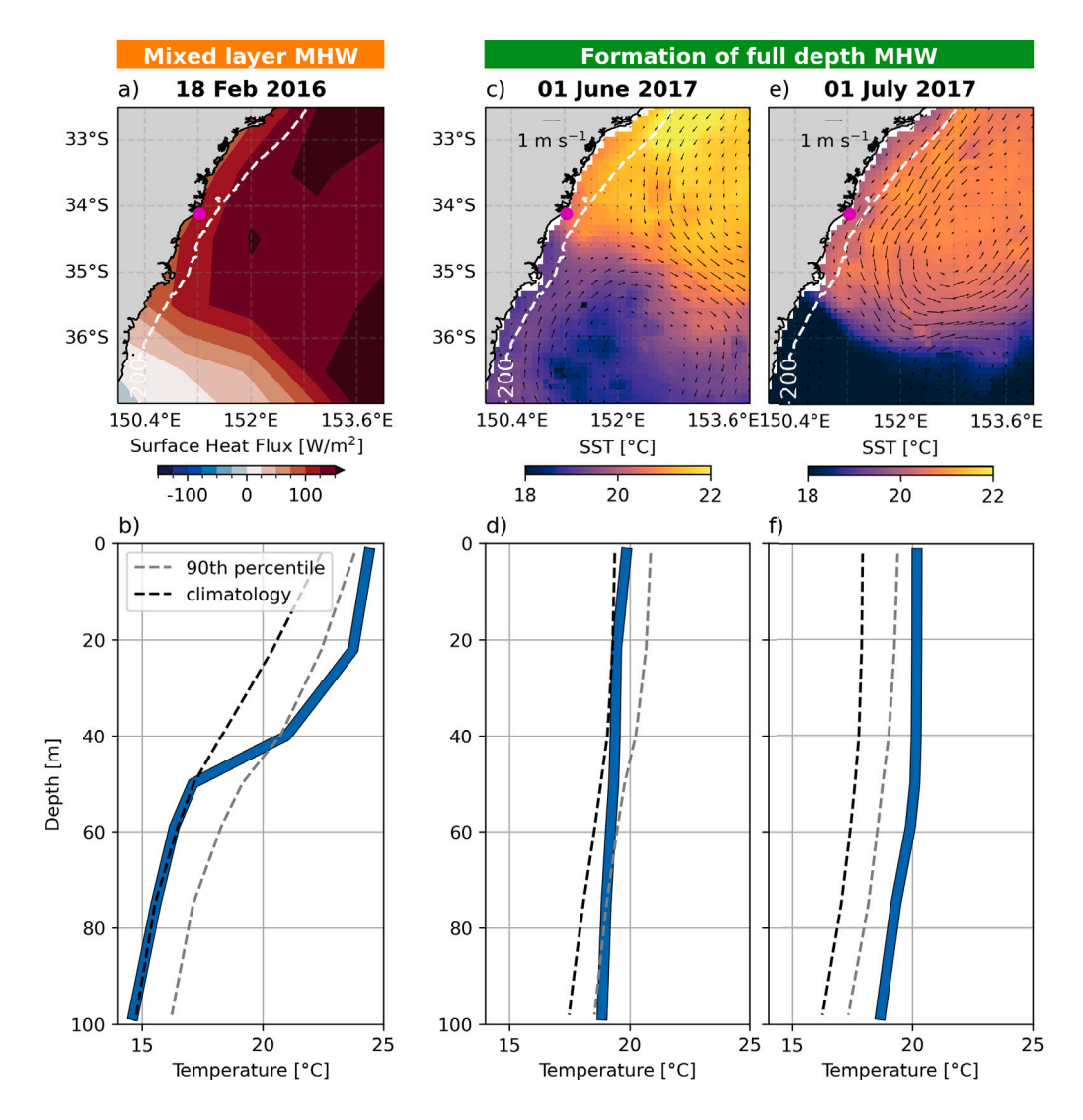


Fig. 8. Comparison at the PH100 mooring site (pink circle at 34 °S) off southeastern Australia between a-b) a mixed layer marine heatwave driven by anomalous air-sea heat fluxes, and c-f) a full depth marine heatwave resulting from the onshore intrusion of the East Australian Current. (a) Shows the total surface heat flux from the ERA5 reanalysis, (b) shows the temperature profile, mean and 90th percentile climatologies from the mooring on 18 February 2016, (c) shows sea surface temperature and geostrophic velocities on 1 June 2017, (e) Sea surface temperature and geostrophic velocities one month later. (d) Vertical temperature profile from the mooring on 1 June 2017, and (f) one month later, showing the development of a full depth marine heatwave.

4.2. Argo case study 1 and 2 - Thermocline MHWs in the tropical Pacific and Indian oceans

In the tropical ocean, thermocline MHWs are common (Hu et al., 2021). The thermocline is often quite shallow and with a sharp vertical temperature gradient, with prominent shifts in thermocline depth associated with wind stress curl driven Ekman pumping and the influence of Kelvin and Rossby wave dynamics. Two examples of different driving mechanisms resulting in thermocline MHWs are presented in Fig. 9. In February 2011, anomalous Ekman pumping (Fig. 9a) caused a depression in the thermocline (Fig. 9b). As a result, warmer temperatures were found deeper than usual in the water column (between 100 and 280 m depth), resulting in a strong thermocline MHW with a severity index as high as 4 at 175 m (the approximate thermocline depth). Fig. 9e shows the clear signature of westward Rossby wave propagation across the tropical Indian Ocean, where raised/lowered sea level anomalies are related to the depression/raising of the thermocline. In early 2007 we see a large positive sea level anomaly that would be associated with a deeper thermocline. At the depth of the mean thermocline, this appears as a strong warming/high severity indicative of a thermocline MHW (Fig. 9d,f). Given the lack of internal heating sources in the ocean

interior and the relatively slow timescales on which interior water masses evolve, many subsurface temperature extremes are likely to be related to the adiabatic redistribution of heat via dynamical processes. Such 'heave' processes can be related to the passage of planetary waves, local wind forcing and Ekman pumping (Fig. 9a), isopycnal movement related to mesoscale eddies (Pegliasco et al., 2015), or large-scale geostrophic adjustment that leads to shifts in oceanic fronts in temperature.

A further diagnostic to help determine mechanisms driving temperature (and salinity) changes in the interior ocean is the Spice and Heave decomposition (Bindoff and Mcdougall, 1994). In the subsurface ocean where vertical mixing is weak, changes in temperature can result from the aforementioned movement of isopycnals (heave) and density compensating temperature and salinity changes occurring along isopycnals (spice). The former is often related to dynamical drivers like Ekman pumping or the passage of planetary waves that cause an adiabatic retribution of temperature as detailed above. The latter relates to water mass changes at the ocean surface that are subsequently transported into the interior via isopycnal mixing or advection. The spice/heave framework was employed by Scannell et al. (2020) to examine the Blob

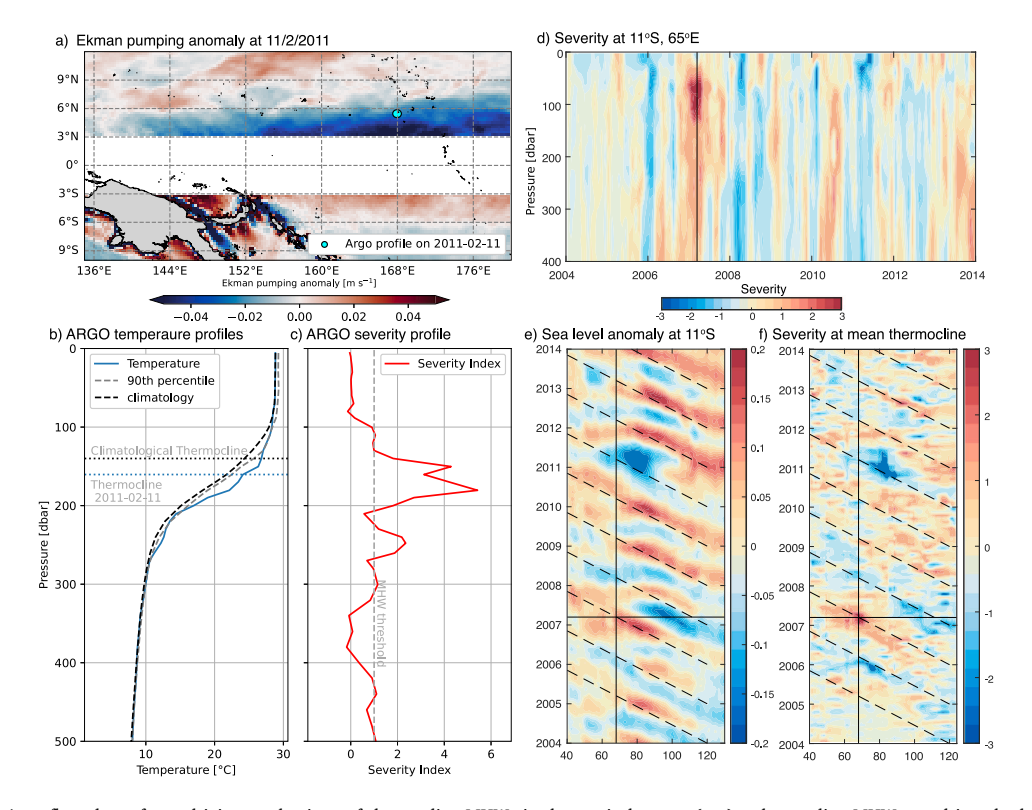


Fig. 9. Examples from Argo float data of two driving mechanisms of thermocline MHWs in the tropical ocean: (a–c) a thermocline MHW was driven by local Ekman pumping in the western tropical Pacific (temperature profile from a single Argo float, threshold calculated from gridded Argo), while the other (d–f) was associated with westward propagating Rossby waves, as indicated by the evolution of sea level anomalies as a function of longitude (x-axis) and time (y-axis) in panel e and severity at mid-thermocline in panel f (sea level anomaly from altimetry, temperature data from gridded Argo).

MHW in the northeastern Pacific. In particular they found that subsurface heating during the Blob was related to entrainment of anomalous heat from the mixed layer to greater depths (a large Spice component), while an earlier subsurface MHW in 2008 was associated with adiabatic deepening of the thermocline (i.e. heave). While potentially useful, isolating the drivers of spice and heave changes can be challenging without additional information and is currently a separate area of research.

5. Ecological impacts of MHW vertical structure

Here, we use an organismal perspective to discuss possible impacts of different distributions of MHWs through the water column. In this context, it is useful to consider a species' ability to move - and hence relocate to suitable habitat outside the impacted depths — when considering ecological impacts of heatwaves (Jacox et al., 2020). The first group we consider are organisms that occupy the benthos — they either live in the sediments or are attached to benthic substrates and have no means of escape from a MHW. Second, there are the planktonic microbes (e.g. bacteria, viruses, phytoplankton) whose distribution is largely determined by ocean currents, which means they largely remain within water masses. Third are those taxa in the pelagic deep scattering layer that vertically migrate up to hundreds of metres per day (zooplankton, mesopelagic fish, and larval fish) and actively move between water masses within the water column. As part of this movement, they will routinely experience relatively large changes in temperature. The last group of organisms are those that have the ability to swim or dive in the unbounded volume of the ocean (fish and marine mammals). Other surface-based organisms such as seabirds are also impacted by MHWs (Piatt et al., 2024) but are not considered here. Given the contrasting mobility and vertical distribution of these four groups of organisms in the ocean, MHW types likely have different relevance and potential consequences.

Mixed layer MHWs

By virtue of occurring in the upper ocean, mixed layer MHWs are expected to have the greatest effect on planktonic microbes and vertical migrators. These organisms move by drifting in ocean currents or vertical migration (Doblin and van Sebille, 2016; Wirtz et al., 2022), and have the potential to be directly physiologically impacted by extreme temperatures or indirectly through vertical stratification and the diminished delivery of nutrients to the photic zone and reduced oxygen availability (e.g. Brown et al. (2024)).

The Blob heatwave in the North Pacific (Bond et al., 2015) is a well known data-rich example of the pelagic implications of a mixed layer MHW. This MHW led to a decline in surface chlorophyll-a, lower primary production, an almost total loss of diatoms (Arteaga and Rousseaux, 2023) and a shift to smaller phytoplankton cells which are harder to consume for many zooplankton (Yang et al., 2018). This drove declines in the abundance of carbon-dense crustacean zooplankton and increases in carbon-poor gelatinous zooplankton (Brodeur et al., 2019a), which then manifested as shifts in the diet of small pelagic fishes as well as declines in their weight and energetic condition (Brodeur et al., 2019b). More generally, Hayashida et al. (2020) and Sen Gupta et al. (2020) showed that MHWs with a surface expression were associated with reduced surface productivity at lower latitudes and elevated surface productivity at higher latitudes as a result of stratification.

Deep MHWs

In addition to the ecological impacts from Mixed Layer MHWs, MHWs with a surface expression that penetrate below the mixed layer will reduce access to cooler refugia in the upper ocean and also expose midwater organisms such as mesopelagic fishes, squids, and crustaceans to elevated temperatures. These organisms are an important source of

food for many large marine top predators, including pinnipeds, sharks, whales and dolphins, and seabirds (Braun et al., 2022; Young et al., 2015). They also provide a significant amount of the daily intake of commercially important pelagic fishes (e.g., tunas, Duffy et al. (2017)). Given that midwater food webs play a key role in transferring and transforming elements between the atmosphere, surface ocean and the deep seafloor (Haddock and Choy, 2024), Deep MHWs could also have significant impacts on global biogeochemical cycles, but observations at depth are lacking. Biogeochemical investigations of the Blob indicate that there were significant increases in surface ocean aragonite saturation state (Ω arag) and decreases in surface dissolved oxygen concentrations that extended to depths of 100 m (Mogen et al., 2022), both of which could have biological implications, such as constraining the depth range of oxygen sensitive tuna and billfish (Prince and Goodyear, 2006). Importantly, depending on the spatial extent and duration of the MHW, midwater predators and prey have the ability to relocate vertically and horizontally in the ocean (Iglesias et al., 2024), limiting their exposure to water outside their thermal optimum. This may come at the cost of increasing their exposure to other predators, or to capture by fisheries.

Thermocline and submerged MHWs

In regards to thermocline MHWs, these are often produced by vertical displacement of water masses (i.e. heave), so planktonic microbes that are passively moved along with the water mass may not experience any change in their ambient condition and biogeochemical impacts may be limited. However, for vertical migrators, thermocline MHWs could have greater consequences through both the direct effects of elevated temperature on their metabolism, but also the indirect effects on prey and predator abundance. Research has suggested that strong Thermocline MHWs resulted in a reduction in the catch of skipjack tuna in the tropical western Pacific. However, the statistical significance of the impact was unclear (Hu et al., 2021).

Benthic MHWs

To date, the most serious and extensive impacts of MHWs have been documented in coastal benthic habitats where benthic organisms such as macroalgae, seagrass, sponges and corals have experienced dieoffs (Arias-Ortiz et al., 2018; Hughes et al., 2018; Arafeh-Dalmau et al., 2019; Holbrook et al., 2021; Bell et al., 2023). Most of the impacted organisms which have been documented exist in shallow well-mixed waters where MHWs detected from the surface are likely to extend all the way to the sea floor. Given that sessile organisms in the benthos of continental shelves and deep ocean basins are just as constrained as shallow water organisms in mobility, it is likely that full depth MHWs will have similar destructive impacts if they are sufficiently intense and prolonged. Deep benthic organisms are exposed to limited temperature variations and already have limits on food acquisition and reproduction imposed on them by their immobility, so they may be particularly vulnerable to MHWs. For deep-sea coral gardens or manganese nodule fields that were formed over thousands of years, the impacts of benthic and full depth MHWs could be very significant in these novel habitats. In particular, loss of habitat-forming foundation species such as corals, seagrass and macroalgae can have significant long-lasting impacts on associated biodiversity, ecological function, and ecosystem services provision (Smith et al., 2024). Following the 2013-2016 MHW in the North Pacific ("The Blob"), there was an unprecedented decline of kelp in northern California (Rogers-Bennett and Catton, 2019). This decline was caused by a combination of direct (MHW) and indirect impacts (increase in urchin predators). The loss of this critical habitat triggered mass abalone mortality and the closure of several recreational and commercial fisheries worth more than \$USD47M (Rogers-Bennett and Catton, 2019). Similar impacts have been seen off the west Australian

coast where a 10 week MHW resulted in extensive macroalgal mortality, an increase in turf-forming algae, and a tropicalisation of the fish community (Wernberg et al., 2013). Even after the return to baseline conditions, these systems are still in recovery and may not return to their original state. Another benthic species not to have recovered following a MHW are the Alaskan snow crab, a \$USD150M industry which collapsed following a Bering Sea MHW (Szuwalski et al., 2023).

Experimental outcomes of MHW simulations with intact sediment cores from the Baltic Sea provide useful insight into how benthic biogeochemistry could be affected (Kauppi and Villnäs, 2022). Short-term (5–9 days) moderate (approx. + 5 °C) and strong (approx. + 9 °C) MHWs have different impacts on biogeochemical cycling of nutrients within the seafloor. Biogeochemical and biological processes were boosted by a moderate heatwave, whereas biogeochemical cycling seemed to decrease under a strong heatwave. A moderate MHW elevated remineralisation but a strong MHW led to decreased microbial processes, resulting in fresh organic material accumulating in the sediments as well as increased metabolism and stress of benthic animals (Kauppi and Villnäs, 2022). The authors noted that the lower oxygen content of warm water at depth may compound any heat-related stress.

Full depth MHWs

Given the usual mechanism of Full Depth MHW formation, frontal movement, this type of MHW may have limited impacts on planktonic microbes — organisms present in the water mass moving to the shelf, as they are just being displaced horizontally. However, with the onshore movement of the warm water, there can be a flow-on effect on coastal ecosystems, as resident species are replaced by warm-adapted organisms from further offshore, as has been observed in the squid fishery on the North Atlantic shelf (Salois et al., 2023). There is also the loss of cooler deeper water as a refuge for the vertical migrators like zooplankton. Additionally, all the threats noted above for the Benthic MHWs will apply equally to Full Depth MHWs where sessile organisms experience the heatwave conditions and have no option to relocate.

6. Data challenges

MHW research has expanded significantly due to long-term, daily near-real-time satellite surface observations globally, allowing for the identification of baseline climatologies and thresholds. However, observing the subsurface ocean is a far greater challenge with few datasets that are near continuous, and that last long enough to accurately represent the variability of temperature in a specific location, let alone globally.

This section discusses the utility and pitfalls of various data products related to our MHW types, summarised in Table A.2, which associates each dataset's characteristics with the MHW types they can detect or classify. Subsurface ocean observations come from platforms with varying coverage: global (Argo floats), regional (expendable bathythermograph [XBT] measurements, animal- and ship-borne instruments), and local (moored instruments and gliders). Temporal coverage ranges from long-term series like Australian coastal moorings since the 1940s (Roughan et al., 2022) to short-term event-based campaigns lasting days to weeks (Lo Bue et al., 2021). Long-term moorings provide excellent platforms for understanding the vertical structure of MHWs at both single (Schaeffer et al., 2023) and multiple locations (He et al., 2024). Moorings provide multivariate data, including salinity and biogeochemical measurements. However, they are location-specific, rarely multidecadal, and the global network suitable for MHW research is limited Most mooring data are only available in delayed mode, hindering real-time assessments needed for adaptive management strategies. Where mooring arrays with real-time capability do exist (e.g. the Coastal Pioneer Mooring Array (Gawarkiewicz et al.,

2020)), they often have short time series due to the cost and complexity of maintaining their deployment.

Most ocean temperature profiles therefore come from autonomous platforms like Argo floats, ocean gliders, and animal-borne sensors equipped with CTD probes (e.g., McMahon et al. (2021)). These resolve vertical temperature variations but lack consistent spatial and temporal coverage for MHW identification and robust climatology. Argo's coverage of continental shelf waters is limited, and animal-borne data may be biased by species' preferences.

The large network of \sim 3000 Argo profiling floats are crucial for subsurface MHW identification in the open ocean, but their short duration hinders robust estimation of high-percentile seasonal climatologies. Studies using Argo data rely on derived gridded products like monthly 1-degree grids (Roemmich and Gilson, 2009). Near-global coverage since 2007 is available for the upper 2000 m, but this limits identification of extremes to those longer than a month. Individual profiles compared to gridded climatology may resolve events at finer timescales (e.g. Fig. 9b), but at the cost of statistical accuracy.

Targeted efforts to measure MHWs in real time include Australia's Integrated Marine Observing System (IMOS) Event-based sampling facility (Benthuysen et al., 2025). Experts determine ocean glider deployments to monitor physical and biogeochemical properties during MHW events in Australia's coastal waters. IMOS gliders captured the 3D structure of a MHW in the Great Barrier Reef in February 2020 (Capotondi et al., 2024). Deployment decisions rely heavily on SST measurements and forecasts, so while they describe the depth structure of MHWs with surface expressions, they cannot compare with MHW thresholds at depth. Continuous glider deployments in key regions are important for monitoring and providing time series and baselines. Combined with appropriate mooring observations, they can provide thresholds or local studies (Malan et al., 2024).

Linking MHWs to subsurface biogeochemical (BGC) changes or identifying subsurface BGC extremes is challenging due to sparse observations. The number of Argo floats with BGC sensors is growing — 644 of 3866 active floats (OceanOps, accessed on 26 July 2024) - providing measurements of dissolved oxygen, nitrate, fluorescence, pH, particles, and irradiance. However, the sparse network and recent deployments make studying extremes challenging.

6.1. Models

Ocean models are valuable for studying MHWs and their typology, providing continuous subsurface output over decades. They include variables like salinity, heat fluxes, and advection for investigating MHW drivers. Models have been used to study surface MHWs (Bian et al., 2023) and subsurface MHWs (Großelindemann et al., 2022). Biogeochemical variables enable studying MHW impacts on BGC and compound events (Gruber et al., 2021; Le Grix et al., 2021). However, models rarely reproduce reality quantitatively; each has unique advantages and limitations, including resolution, surface forcings, data assimilation, coupling, and representation of temperature extremes.

The MHW definition may need adaptation based on dataset limitations, available diagnostics, temporal extent, and sampling rate. Storage constraints force modellers to trade off between dataset duration and resolution, especially at high resolution. High-dimensional data like global eddy-resolving 3D daily temperature over 30 years is rare. Daily outputs are usually limited to 2D fields (e.g., SST), with 3D fields saved monthly. Models may include diagnostics (e.g., surface fluxes) providing insight into MHW mechanisms, but ambiguity remains due to incomplete stored diagnostics computed at the sufficiently high time resolution required to close the heat budget (Yung and Holmes, 2023).

Global ocean models used for MHW studies include surface-forced free-running models, coupled free-running models, and ocean reanalyses and state estimates. Free-running coupled global climate models may span centuries but usually have low resolution (typically 1°; Chen

et al. (2021)) and coarse temporal sampling. They capture atmosphereocean feedbacks but suffer from biases and drifts without data assimilation, cannot reproduce individual observed MHW events, and
parameterise eddy heat transports. Higher-resolution free-running coupled global ocean-sea ice models driven by prescribed surface forcing
(e.g., ACCESS-OM2-01; Pilo et al. (2019)) may represent MHWs related
to mesoscale processes but lack data assimilation. They may have
realistic MHW statistics but cannot capture specific observed events
driven by internal processes. If driven by data-assimilated atmospheric
datasets (e.g., JRA55-do, ERA5), they may capture MHWs driven by
surface forcing or atmosphere-forced dynamics but may exaggerate the
role of surface forcing due to lack of feedback (e.g. a prescribed atmosphere acts as though it has infinite heat capacity). These models allow
quantitative investigation of MHW mechanisms if sufficient diagnostics
are available.

Finally, ocean reanalyses provide gap-free, gridded subsurface data approximating observed ocean features but most suffer from "assimilation shock", losing dynamical balance at each assimilation step. While useful for identifying and classifying observed MHWs and understanding their evolution, uncertainties in heat budgets may be too large for meaningful analysis. Ocean state estimates (e.g. ECCO, Forget et al. (2015)) allow data assimilation while maintaining dynamical balances. making them suitable for budget analysis. However, the relatively high computational cost of ocean state estimates restricts both their availability and resolution. For both reanalyses and ocean state estimates, the same spatial and temporal challenges apply as with observational data, with most assimilated data being surface observations. Ocean models' limitations are defined by their ability to represent different scales of variability. Based on grid resolution and parameterisation, models can be eddy-rich (0.1°, 0.01°), eddy-permitting (0.25°), or omit meso- and sub-mesoscale processes (1°). Higher resolution results in better representation of heat and energy conversions between scales, and more realistic vertical heat motions driven by fronts and eddies, important in MHW dissipation or propagation. Eddy-resolving models require fewer parameterisations and better represent ocean circulation features linked to heat distribution, showing less bias (Pilo et al., 2019). When analysing model output in MHW studies, understanding the model's ability to represent temperature extremes is crucial. Comparing modelled temperatures to observations, including means, standard deviations, and percentiles, helps identify biases. Comparing MHW metrics between models and observations provides insights into accuracy. In global coupled models, assessing their ability to simulate modes of variability driving major MHWs is important.

Identification of MHWs with depth with the wide variety of data sources outlined above presents a significant challenge, requiring dedicated investigation. Schlegel et al. (2019) demonstrated a robust statistical approach showing the trade-offs to be considered when detecting MHWs from sub-optimal data. They demonstrated that datasets as short as 10 years in duration and with up to 25% missing data (50% if interpolation is used) can still produce reasonable MHW metrics, with the caveat that it is important to perform post-hoc uncertainty estimates when comparing datasets. Many studies have also used monthly data for the study of MHWs, especially long-lasting events. Subsurface events can have enhanced persistence (Scannell et al., 2020; Elzahaby et al., 2025), justifying the use of monthly averaged data in some cases (e.g. our Figs. 3c and Fig. 9), although the implications of these choices must be considered and communicated carefully.

7. Discussion

In this work we have presented a refined typology for the vertical structure of marine heatwaves. We highlight the importance of using the mixed layer and thermocline depths to reference the depth of marine heatwaves, and the importance of accounting for changes in temperature variability with depth using the marine heatwave severity index.

Using these principles we identified the vertical structure of six MHW types; Mixed layer MHWs, Deep MHWs, Thermocline MHWs, Full Depth MHWs, Submerged MHWs and Benthic MHWs. These 6 types provide the language needed to describe the vertical marine heatwave structure across a variety of datasets, from a single coastal mooring to extreme temperature profiles in a global ocean model. Our typology integrates knowledge from previous studies on subsurface MHWs and generalises it to be applicable in a wide range of ocean depths, datasets and dynamic regimes. We note that MHWs are known to evolve in their vertical extent over time, and our typology allows for this evolution to be described as a particular event transitions from one type to another over time. Our approach of describing the vertical structure of MHWs on a profile-to-profile basis helps to simplify the challenge of Lagrangian vs Eulerian characterisation of MHW structure pointed out by Gruber et al. (2021).

How our typology helps process-based science — identifying drivers

The mixed layer and thermocline present important barriers for both physical and biological dynamics. To describe the vertical extent of MHWs simplifies the process of identifying the drivers of specific MHW events. We show that specific drivers can be responsible for different types of events, for example surface heat fluxes are typically associated with mixed layer MHWs, while Ekman pumping is usually related to thermocline MHWs.

Different MHW types may have different impacts — why this is important

Most importantly, different vertical marine heatwave structures can result in different biological and biogeochemical impacts, especially when considering differing abilities of some organisms to vertically migrate or relocate to thermal refugia. Different types of MHWs may also result in increased or reduced supply of nutrients to the euphotic zone due to the changes in stratification driven by different MHW types. We believe our typology simplifies the process of associating a MHW event with its impacts, thus enabling the interdisciplinary research that is at the core of the study of MHWs. Of course, while this typology allows us to describe MHW vertical structure and how it evolves over time, it does not take into account either the change in the environment at a specific location in space, nor the shrinking of a particular suitable habitat due to warming. It is clear that the duration, intensity and spatial coverage of a MHW will be critical to determining actual ecological effects. Currently, we have very limited data that fully documents the impact of MHWs but it is not unreasonable to expect that they could have devastating consequences. A high priority for research will be to advance understanding of the prevalence and predictability of subsurface MHWs and their impacts by undertaking surveys in highvalue or novel habitats before and after such events. Several studies have shown skill in the prediction of surface MHWs (McAdam et al., 2023; Smith et al., 2024). The predictability and prediction skill of subsurface MHW intensities and vertical profiles also need to be investigated. MHW prediction models often only provide surface or whole water column estimates, so we suggest that there should be a future move to also forecasting subsurface MHWs based on our classification.

High commercial value mobile species that primarily occupy upperocean habitats (the epipelagic and upper mesopelagic), such as tunas, mackerel, anchoveta, herring, and billfishes may be used as sentinel taxa for understanding MHW impacts on marine resources. As MHWs become more frequent, countries will face new management challenges as pelagic species with the ability to move are redistributed into new areas (either into the unregulated High Seas or into different Exclusive Economic Zones) and fishing fleets follow them. This will create episodic fishing and tourism opportunities, but also threats to protected or unregulated species in these new areas (Welch et al., 2023; Farchadi et al., 2024). Due to the fact that many of these species feed at depth, the growing body of evidence that a large proportion of MHWs are not visible from the surface must be taken into account if MHW statistics are to be used as part of any management strategy. As such, recent observational programmes (Manning et al., 2009; Lago et al., 2025) which collaborate with the fishing industry to collect subsurface temperature data are a welcome development.

8. Conclusion

MHW research has succeeded in stimulating inter-disciplinary work, as it provides a common language (the MHW definition) that can be used across different locations and disciplines. The definition is simple, but allows events to be described using only a few metrics. As a next step, we have extended this common language to the subsurface, to enable interdisciplinary research and gain understanding of the impacts of different vertical distributions of marine heatwaves. Vertical scales are much smaller than horizontal scales, and arguably have greater biological impact. Using a MHW typology allows different vertical structures to be discussed and described, including their evolution in time and space, without the physics becoming too complex to inhibit our understanding of impact.

CRediT authorship contribution statement

Neil Malan: Software, Methodology, Visualization, Conceptualization, Writing - original draft, Formal analysis, Writing - review & editing, Investigation. Alex Sen Gupta: Writing - review & editing, Funding acquisition, Writing - original draft, Conceptualization, Methodology, Software, Visualization. Amandine Schaeffer: Writing - review & editing, Writing - original draft, Conceptualization, Investigation, Methodology. Shujing Zhang: Writing - original draft, Visualization, Writing - review & editing, Investigation, Methodology, Software. Martina A. Doblin: Writing - review & editing, Writing - original draft, Conceptualization, Methodology. Gabriela Semolini Pilo: Writing review & editing, Conceptualization, Methodology, Writing - original draft. Andrew E. Kiss: Writing - review & editing, Conceptualization, Writing - original draft, Data curation, Investigation, Methodology. Jason D. Everett: Writing - review & editing, Investigation, Methodology, Writing – original draft, Erik Behrens: Conceptualization, Writing - review & editing. Antonietta Capotondi: Conceptualization, Writing - review & editing. Sophie Cravatte: Writing - review & editing, Conceptualization. Alistair J. Hobday: Conceptualization, Writing review & editing. Neil J. Holbrook: Writing - review & editing, Conceptualization. Jules B. Kajtar: Conceptualization, Writing - review & editing. Claire M. Spillman: Conceptualization, Writing - review & editing.

Declaration of competing interest

The authors declare the following financial interests/personal relationships which may be considered as potential competing interests: Neil Malan reports financial support, article publishing charges, and travel were provided by Australian Research Council. Alex Sen Gupta reports financial support was provided by Australian Research Council. Gabriela Semolini Pilo reports financial support was provided by Integrated Marine Observing System. Neil J Holbrook reports financial support was provided by Australian Research Council. Erik Behrens reports financial support was provided by National Institute of Water and Atmospheric Research. Antionetta Capotondi reports financial support was provided by NOAA Climate Program Office. Antionetta Capotondi reports financial support was provided by NASA. Sophie Cravatte reports financial support was provided by Institut de Recherche pour le development. If there are other authors, they declare that they have no known competing financial interests or personal relationships that could have appeared to influence the work reported in this paper.

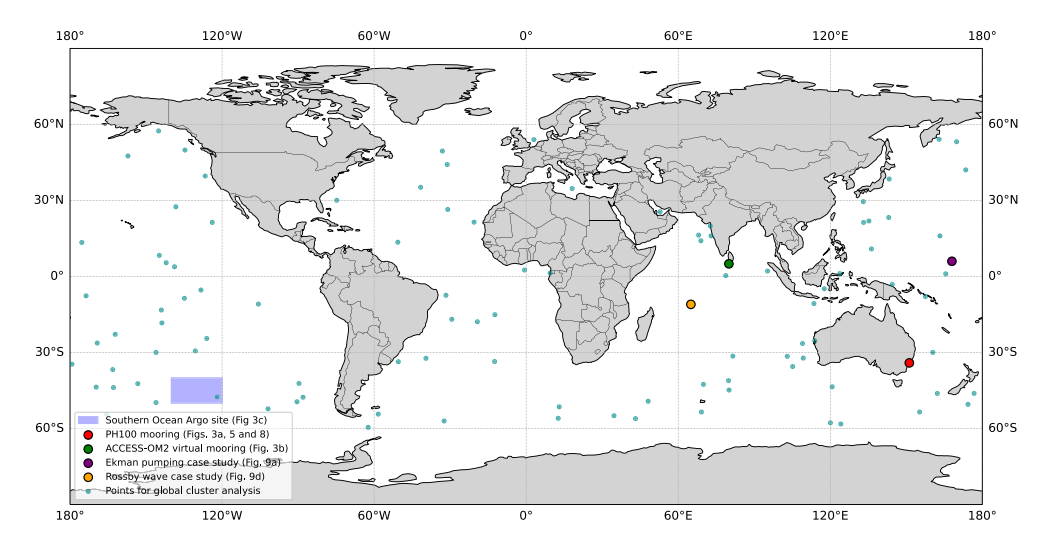


Fig. A.10. Map showing the location of analysis sites discussed in the text.

Acknowledgements

NM and ASG are supported by an Australian Research Council Future Fellowship (FT220100475). AEK is supported by Australian Research Council grant LP200100406. The ACCESS-OM2-01 model runs and analysis were undertaken with computational resources provided by the Australian Government through the National Computational Infrastructure (NCI) under the National Computational Merit Allocation Scheme and ANU Merit Allocation Scheme. We thank the Consortium for Ocean–Sea Ice Modelling in Australia for making the outputs of the ACCESS-OM2 suite of models available through the NCI. GSP is supported by Australia's Integrated Marine Observing System (IMOS) - IMOS is enabled by the National Collaborative Research Infrastructure Strategy (NCRIS). NJH is supported by the Australian Research Council Centre of Excellence for Climate Extremes (CE170100023) and the National Environmental Science Program Climate Systems Hub. EB is supported through the National Institute of Water and Atmospheric

Research Strategic Science Investment Fund to Coasts and Estuaries Science Centre (CEME2506). A.C. was supported by the NOAA Climate Program Office's MAPP program, and NASA Physical Oceanography grant #80NSSC21K0556. S.C. was supported by IRD in the framework of the MaHeWa project funded by the French National Research Agency under France 2030 (ANR-23-POCE-0001), and by the Fonds Pacifique in the framework of the HEAT project. This manuscript was originally conceived and early concepts developed at a three-day workshop cosponsored by the ARC Centre of Excellence for Climate Extremes and the CLIVAR Research Focus on Marine Heatwaves in the Global Ocean.

Appendix A. Map of all analysis sites

See Fig. A.10.

Table A.1

Cluster characteristics from the global ACCESS-OM2-01 cluster analysis presented in Fig. 4. Medians and interquartile ranges (in parentheses) are presented for the MLD, thermocline depth, maximum severity index with depth, maximum intensity (°C above the climatological mean) with depth, and the intensity at the depth of maximum severity. These statistics are computed for the profiles in each cluster (a–e from Fig. 4). This table includes five cluster types; the sixth type (Benthic) is a coastal variation.

	Mixed layer	Deep	Thermocline	Full Depth	Submerged
Members of cluster	4542	3754	2882	7348	6592
MLD [m]	32	50	35	50	37
	(18–55)	(21–105)	(17–76)	(29–94)	(19–69)
Thermocline Depth [m]	98	121	150	135	121
	(78–135)	(78–186)	(109–207)	(70–254)	(78–186)
Maximum Severity with depth	2.34	2.58	2.34	2.45	2.35
	(2.16–2.63)	(2.23–3.11)	(2.14–2.76)	(2.18–2.96)	(2.15–2.68)
Maximum Intensity with depth [°C]	1.30	1.66	1.60	1.24	0.72
	(1.00–1.84)	(1.15–2.34)	(1.15–2.48)	(0.75–2.04)	(0.41–1.35)
Intensity at depth of maximum severity [°C]	1.18	1.46	1.41	0.41	0.33
	(0.93–1.61)	(0.95–1.98)	(0.94–2.06)	(0.20–1.35)	(0.20–0.69)

Table A.2

Datasets available for subsurface MHW work

Buttisets uvuria	DIC 101 SUDSUITUCE 14	IIIII WOIK.							
Dataset	Type of MHWs detectable	Coverage (Space)	Coverage (Time)	Resolution (space)	Resolution (time)	Advantages	Disadvantages	Comment	Reference
Satellite sea surface temperature (SST)	Mixed layer, deep, full-depth coastal and open-ocean	Global	30–40 years	Horizontal: 0.1-0.25° (gap-free); ~100m-km (infra-red) Vertical: N/A	Daily (gap-free); hours (infra-red))	Near real time. Long enough to establish climatology Near continuous view of temperature in gap-free products.	- No subsurface Discrepancies between different satellite products.	Different products measure different properties e.g. skin vs. foundation temperature.	SST intercomparisons: Huang et al. (2023) NOAA-OI: Reynolds et al. (2007) CCI: Merchant et al. (2019)
Satellite Altimetry	mostly deep, full-depth or mixed layer open-ocean	Global	1994–present (for multi-satellite gridded product)	Horizontal (multi-satellite gridded product): 0.25° Vertical: N/A	Daily (interpolated)	Near real time. Indicative of integrated heat content	 No subsurface Not temperature directly. Link through steric height. 	Provides indirect evidence of subsurface heat over the water column.	AVISO IMOS (Australia)

(continued on next page)

Table A.2 (continued).

Dataset	Type of MHWs detectable	Coverage (Space)	Coverage (Time)	Resolution (space)	Resolution (time)	Advantages	Disadvantages	Comment	Reference
Argo profilers	ALL but benthic open-ocean	Near Global (> 3800 worldwide), 0-2000 m depth	2004–present	Horizontal: N/A; 0.5° (gridded product) Vertical: ~2 m bins over 0-2000 m or 0-4000/6000 m for deep floats.	Profiles every 10 days; Monthly gridded product	Near real time. Depth structure resolved with high vertical resolution. Measurements of temperature, salinity. Available as a gridded product.	Observations are still sparse. No measurements on the shelf. Sometimes misses near-surface measurements. Too short to establish a robust climatology. Daily variability not resolved.	Established ideal coverage of 2 floats per 3° square; Core and Deep Argo measure temperature and salimity; BGC Argo floats can also measure dissolved oxygen, pH, nitrate, backscatter, fluorescence, and downwelling light.	Argo: Argo gridded products: Roemmich and Gilson (2009).
Moorings	ALL coastal and open-ocean	Local	Years/decades (rare)	Horizontal: N/A Vertical: ~1 m	Very high frequency ~minutes/days	- High temporal resolution - Depth structure resolved with high vertical resolution - On shelf measurements - Multiple variables available (mooring dependent).	Very sparse. Limited number of long time series for climatology. Problems with continuity with sensor failures or service.	A few datasets offer multi-decadal records. Often include bottom temperature information.	Bailey et al. (2019)
Data Loggers	ALL coastal	Local	Months-years	Generally in shallow locations	Variable frequency depending on duration deployed and on-board storage	- May have telemetry capability - Cost effect - Useful for embayment's/lagoons	- Sparse - Temperature only - May only have delayed data retrieval		E.g. Ridgway and Ling (2023)
Ocean gliders	ALL coastal and open-ocean	Regional	Days-weeks	Horizontal: ~km Vertical: ~1 m over 0~200 m or 0~1000 m.	High frequency	- Near real time Depth structure resolved with high vertical resolution - Can be deployed on short notice (e.g. for MHW process studies) - Multiple variables available (temperature, salinity, fluorescence, dissolved oxygen, depth-integrated currents).	Moving platform Climatologies are difficult due to being sparse in time. Limited control of location	Can include bottom temperature information.	Testor et al. (2019)
Expendable Bathythermo- graph (XBT)	ALL coastal and open-ocean	Local	Snapshot to decades	Horizontal: N/A; km along lines Vertical: ~1 m over 0–800 m.	Snapshot in time; some lines are repeated quarterly or less frequently.	- Depth structure resolved with high vertical resolution - Most subsurface - observations prior to Argo Can be deployed from a ship of opportunity.	- Climatologies require care due to being sparse in time.	Generally along shipping lines	Cowley et al. (2013)
Conductivity – Temperature – Depth (CTD)	ALL coastal and open-ocean	Local	Snapshot to decades	Horizontal: N/A; km along lines Vertical: ~1 m	Snapshot in time	- Depth structure resolved with high vertical resolution - High precision - Multiple variables available (temperature, salinity, often fluorescence, dissolved oxygen).	- Rare climatology due to being sparse in time. - Requires research vessel deployment - Only measurement reaching 5,000 m depth.	Can include bottom temperature information.	
Animal borne sensors	ALL coastal and open-ocean	Regional	Snapshot to years	Horizontal: N/A Vertical: ~1 m	High frequency depending on animal movement	- Measurements in hard to reach areas, e.g. below ice. - Targets biologically important regions - Multiple variables (salinity)	- No control on location - Sparse - No climatology	Usually a CTD attached to an animal. Profiles from animal dive, and measurements along horizontal trajectory	IMOS Seal CTD Hussey et al. (2015)
Reanalyses and state estimates (i.e., surface-forced models with data assimilation)	ALL open-ocean	Global	Multi-decadal	Multiple resolutions available (including eddy-resolving)	Typically daily/monthly	- Spatially/temporally continuous - Constrained by available observations - All physical variables (some include BGC)	Not dynamically balanced apart from rare state estimates Large differences between reanalysis products Least constrained in the subsurface		BRAN GODAS SODA ECCO EN4 as used by Sun et al. (2023)
Forced ocean and ocean-sea ice models OGCM	ALL open-ocean	Global	Decadal– centennial	Multiple resolutions available (including eddy-resolving)	Typically daily/monthly (depending on application/stor- age availability)	- Constrained by atmospheric fluxes - May include BGC - Ability to run bespoke experiments - Possibility of multiple ensembles to capture internal variability	- Not constrained by ocean observation, so will not capture specific events unless driven by the surface forcing - No feedback with atmosphere		

(continued on next page)

Table A.2 (continued).

Dataset	Type of MHWs detectable	Coverage (Space)	Coverage (Time)	Resolution (space)	Resolution (time)	Advantages	Disadvantages	Comment	Reference
Climate Models	ALL open-ocean	Global	Decadal - centennial	Typically 1deg ocean resolution	Typically archived monthly (with some daily data)	- Internally consistent - Large number of models - Ability to examine future scenarios - Multiple ensembles often available - May include BGC - Ability to run bespoke experiments	Coarse resolution Often have large biases Variability does not co-vary with real world Heavily parametrised Poorly resolved bathymetry		
Regional Ocean Models	ALL coastal and open-ocean	Regional	Yearly-decadal	Eddy- submesoscale resolutions	Depends on application.	- Targeted at specific applications/regions - Can simulate coastal/shelf regions - May include BGC - Ability to run bespoke experiments	- Contains biases (including those inherited from parent model)		

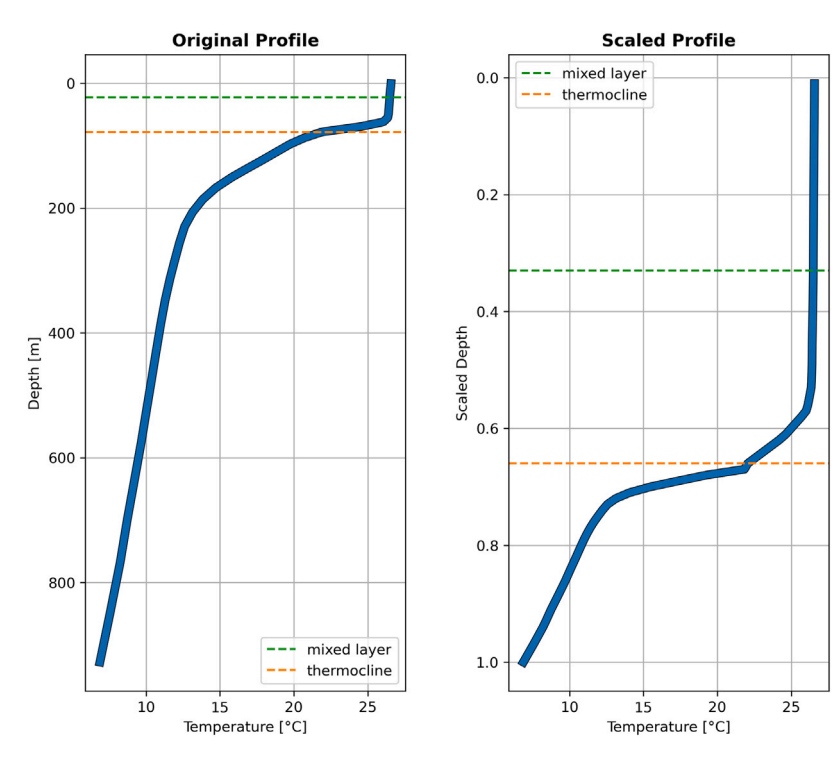


Fig. B.11. An example of a water column which has been rescaled by mixed layer and thermocline depth.

Appendix B. Global clustering of marine heatwave profiles methodology

Steps followed for global clustering analysis:

- Take a large number of randomly selected, dynamically consistent, temperature profiles from an ocean model a 20-year long time series at 100 sites randomly distributed around the global ocean.
- Calculate climatologies, MHW thresholds, anomalies, and MHW severity index at each point, as well as the mixed layer and thermocline depths.
- Separate out profiles which contain an MHW severity index > 2 somewhere in the water column.
- Rescale the depths of each profile using the time-varying mixed layer and thermocline so that each water column can be directly compared, regardless of depth.
- · Concatenate all 100 time series into a single array.
- Use agglomerative clustering from scikit-learn to split the vertical MHW structures into composites, using ward linkage.

• The same steps are followed for the coastal mooring clustering, but using profiles with a severity >1.

Rescaling of profiles

We rescale the profiles, using the natural dynamical and biological boundaries of the mixed layer and the thermocline on each day as our points of reference. This allows an 'apples with apples' comparison of profiles within a time series, and has the secondary benefit of enabling the comparison of the distribution of extreme temperatures in water columns of vastly different depth. An example of this rescaling can be seen in Fig. B.11.

We rescale by interpolating each profile onto a new vertical grid. Firstly, we interpolate the data onto a 1 m vertical grid. Then we define a new depth coordinate, with values ranging from 0 (the surface) to 1 (the ocean floor or the bottom of our data). The first third of this water column (from 0 to 0.33) is populated with the temperature from the surface to the base of the daily-varying mixed layer. The second third (0.33 to 0,66) is populated by the data from the base of the daily-varying mixed layer to the daily-varying thermocline depth. The remainder of the water column (0.66 to 1) is populated with data

from the daily-varying thermocline to the ocean floor or bottom of the dataset.

In order to prevent the extrapolation of data in cases where the thermocline is very close to the mixed layer depth, we adjust the thermocline to be at least 10 m below the base of the mixed layer. This also helps deal with edge cases in the high latitudes where the thermocline may be shallower than the mixed layer.

Data availability

All data used in this paper is publicly available.

References

- Amaya, D.J., Jacox, M.G., Alexander, M.A., Scott, J.D., Deser, C., Capotondi, A., Phillips, A.S., 2023. Bottom marine heatwaves along the continental shelves of North America. Nat. Commun. 14 (1), 1–15. http://dx.doi.org/10.1038/s41467-023-36567-0.
- Amaya, D.J., Miller, A.J., Xie, S.-P., Kosaka, Y., 2020. Physical drivers of the summer 2019 North Pacific marine heatwave. Nat. Commun. 11 (1), 1903. http://dx.doi. org/10.1038/s41467-020-15820-w.
- Arafeh-Dalmau, N., Montaño-Moctezuma, G., Martínez, J.A., Beas-Luna, R., Schoeman, D.S., Torres-Moye, G., 2019. Extreme marine heatwaves Alter Kelp forest community near its equatorward distribution limit. Front. Mar. Sci. 6, http://dx.doi.org/10.3389/fmars.2019.00499.
- Arias-Ortiz, A., Serrano, O., Masqué, P., Lavery, P.S., Mueller, U., Kendrick, G.A., Rozaimi, M., Esteban, A., Fourqurean, J.W., Marbà, N., Mateo, M.A., Murray, K., Rule, M.J., Duarte, C.M., 2018. A marine heatwave drives massive losses from the world's largest seagrass carbon stocks. Nat. Clim. Chang. 8 (4), 338–344. http://dx.doi.org/10.1038/s41558-018-0096-y.
- Arteaga, L.A., Rousseaux, C.S., 2023. Impact of Pacific Ocean heatwaves on phyto-plankton community composition. Commun. Biol. 6 (1), 1–13. http://dx.doi.org/10.1038/s42003-023-04645-0.
- Bailey, K., Steinberg, C., Davies, C., Galibert, G., Hidas, M., McManus, M.A., Murphy, T., Newton, J., Roughan, M., Schaeffer, A., 2019. Coastal mooring observing networks and their data products: Recommendations for the next decade. Front. Mar. Sci. 6, http://dx.doi.org/10.3389/fmars.2019.00180.
- Bell, J.J., Smith, R.O., Micaroni, V., Strano, F., Balemi, C.A., Caiger, P.E., Miller, K.I., Spyksma, A.J.P., Shears, N.T., 2023. Marine heat waves drive bleaching and necrosis of temperate sponges. Curr. Biol. 33 (1), 158–163.e2. http://dx.doi.org/ 10.1016/j.cub.2022.11.013.
- Benthuysen, J.A., Pattiaratchi, C., Spillman, C.M., Govekar, P., Beggs, H., de Oliveira, H.B., Chandrapavan, A., Feng, M., Hobday, A.J., Holbrook, N.J., Jaine, F.R., Schaeffer, A., 2025. Observing marine heatwaves using ocean gliders to address ecosystem challenges through a coordinated national program. Oceanography 38 (1), 22–25. http://dx.doi.org/10.5670/oceanog.2025e101.
- Bian, C., Jing, Z., Wang, H., Wu, L., Chen, Z., Gan, B., Yang, H., 2023. Oceanic mesoscale eddies as crucial drivers of global marine heatwaves. Nat. Commun. 14 (1), 2970. http://dx.doi.org/10.1038/s41467-023-38811-z.
- Bindoff, N.L., Mcdougall, T.J., 1994. Diagnosing climate change and ocean ventilation using hydrographic data. J. Phys. Oceanogr. 24 (6), 1137–1152. http://dx.doi.org/10.1175/1520-0485(1994)024<1137:DCCAOV>2.0.CO;2.
- Bond, N.A., Cronin, M.F., Freeland, H., Mantua, N., 2015. Causes and impacts of the 2014 warm anomaly in the NE Pacific. Geophys. Res. Lett. 42 (9), 3414–3420. http://dx.doi.org/10.1002/2015GL063306.
- Braun, C.D., Arostegui, M.C., Thorrold, S.R., Papastamatiou, Y.P., Gaube, P., Fontes, J., Afonso, P., 2022. The functional and ecological significance of deep diving by large marine predators. Annu. Rev. Mar. Sci. 14, 129–159. http://dx.doi.org/10.1146/ annurev-marine-032521-103517.
- Brodeur, R.D., Auth, T.D., Phillips, A.J., 2019a. Major shifts in pelagic micronekton and macrozooplankton community structure in an upwelling ecosystem related to an unprecedented marine heatwave. Front. Mar. Sci. 6, http://dx.doi.org/10.3389/ fmars.2019.00212, Publisher: Frontiers.
- Brodeur, R.D., Hunsicker, M.E., Hann, A., Miller, T.W., 2019b. Effects of warming ocean conditions on feeding ecology of small pelagic fishes in a coastal upwelling ecosystem: a shift to gelatinous food sources. Mar. Ecol. Prog. Ser. 617–618, 149–163. http://dx.doi.org/10.3354/meps12497.
- Brown, M.V., Ostrowski, M., Messer, L.F., Bramucci, A., van de Kamp, J., Smith, M.C., Bissett, A., Seymour, J., Hobday, A.J., Bodrossy, L., 2024. A marine heatwave drives significant shifts in pelagic microbiology. Commun. Biol. 7 (1), 1–14. http: //dx.doi.org/10.1038/s42003-023-05702-4.
- Capotondi, A., Newman, M., Xu, T., Di Lorenzo, E., 2022. An optimal precursor of Northeast Pacific marine heatwaves and central Pacific El Niño events. Geophys. Res. Lett. 49 (5), http://dx.doi.org/10.1029/2021GL097350, e2021GL097350.

- Capotondi, A., Rodrigues, R.R., Sen Gupta, A., Benthuysen, J.A., Deser, C., Frölicher, T.L., Lovenduski, N.S., Amaya, D.J., Le Grix, N., Xu, T., Hermes, J., Holbrook, N.J., Martinez-Villalobos, C., Masina, S., Roxy, M.K., Schaeffer, A., Schlegel, R.W., Smith, K.E., Wang, C., 2024. A global overview of marine heatwaves in a changing climate. Commun. Earth Env. 5 (1), 1–17. http://dx.doi.org/10.1038/s43747.024.018.06.9
- Chen, K., Gawarkiewicz, G., Kwon, Y.-O., Zhang, W.G., 2015. The role of atmospheric forcing versus ocean advection during the extreme warming of the northeast U.S. continental shelf in 2012. J. Geophys. Res.: Ocean. 120, 4324–4339. http://dx.doi.org/10.1002/2014JC010547.
- Chen, D., Rojas, M., Samset, B.H., Cobb, K., Diongue-Niang, A., Edwards, P., Emori, S., Faria, S.H., Hawkins, E., Hope, P., Huybrechts, P., Meinshausen, M., Mustafa, S.K., Plattner, G.-K., Tréguier, A.M., 2021. Framing, context, and methods. In: Masson-Delmotte, V., Zhai, P., Pirani, A., Connors, S.L., Péan, C., Berger, S., Caud, N., Chen, Y., Goldfarb, L., Gomis, M.I., Huang, M., Leitzell, K., Lonnoy, E., Matthews, J.B.R., Maycock, T.K., Waterfield, T., Yelek, ci, O., Yu, R., Zhou, B. (Eds.), Climate Change 2021: the Physical Science Basis. Contribution of Working Group I To the Sixth Assessment Report of the Intergovernmental Panel on Climate Change. Cambridge University Press, Cambridge, United Kingdom and New York, NY, USA, pp. 147–286. http://dx.doi.org/10.1017/9781009157896.001.
- Cowley, R., Wijffels, S., Cheng, L., Boyer, T., Kizu, S., 2013. Biases in expendable bathythermograph data: A new view based on historical side-by-side comparisons. J. Atmos. Ocean. Technol. 30 (6), 1195–1225. http://dx.doi.org/10.1175/JTECH-D-12-00127.1.
- Cullen, J.J., 2015. Subsurface chlorophyll maximum layers: Enduring enigma or mystery solved? Annu. Rev. Mar. Sci. 7, 207–239. http://dx.doi.org/10.1146/annurevmarine-010213-135111.
- de Boyer Montégut, C., Madec, G., Fischer, A.S., Lazar, A., Iudicone, D., 2004. Mixed layer depth over the global ocean: An examination of profile data and a profilebased climatology. J. Geophys. Res. Ocean. 109 (12), 1–20. http://dx.doi.org/10. 1029/2004JC002378.
- Deng, X., Griffin, D.A., Ridgway, K., Church, J.A., Featherstone, W.E., White, N.J., Cahill, M., 2011. Satellite altimetry for geodetic, oceanographic, and climate studies in the Australian region. In: Coastal Altimetry. Springer Berlin Heidelberg, Berlin, Heidelberg, pp. 473–508.
- Doblin, M.A., van Sebille, E., 2016. Drift in ocean currents impacts intergenerational microbial exposure to temperature. Proc. Natl. Acad. Sci. 113 (20), 5700–5705. http://dx.doi.org/10.1073/pnas.1521093113.
- Duffy, L.M., Kuhnert, P.M., Pethybridge, H.R., Young, J.W., Olson, R.J., Logan, J.M., Goñi, N., Romanov, E., Allain, V., Staudinger, M.D., Abecassis, M., Choy, C.A., Hobday, A.J., Simier, M., Galván-Magaña, F., Potier, M., Ménard, F., 2017. Global trophic ecology of yellowfin, bigeye, and albacore tunas: Understanding predation on micronekton communities at ocean-basin scales. Future of oceanic animals in a changing ocean, Deep. Sea Res. Part II: Top. Stud. Ocean. Future of oceanic animals in a changing ocean, 140, 55–73.http://dx.doi.org/10.1016/j.dsr2.2017.03.003,
- Dutheil, C., Lal, S., Lengaigne, M., Cravatte, S., Menkès, C., Receveur, A., Börgel, F., Gröger, M., Houlbreque, F., Le Gendre, R., Mangolte, I., Peltier, A., Meier, H.E.M., 2024. The massive 2016 marine heatwave in the Southwest Pacific: An "El Niño–Madden-Julian oscillation" compound event. Sci. Adv. 10 (41), http://dx.doi.org/10.1126/sciadv.adp2948, eadp2948.
- Elzahaby, Y., Delaux, S., Schaeffer, A., Roughan, M., 2025. Self-organising maps reveal distinct spatial and temporal patterns in the build-up of marine heatwaves in the Tasman Sea. Ocean. Dyn. 75 (2), 16. http://dx.doi.org/10.1007/s10236-025-01660z.
- Elzahaby, Y., Schaeffer, A., 2019. Observational insight into the subsurface anomalies of marine heatwaves. Front. Mar. Sci. 6, http://dx.doi.org/10.3389/fmars.2019.00745.
- Elzahaby, Y., Schaeffer, A., Roughan, M., Delaux, S., 2022. Why the mixed layer depth matters when diagnosing marine heatwave drivers using a heat budget approach. Front. Clim. 4, http://dx.doi.org/10.3389/fclim.2022.838017.
- Farchadi, N., Welch, H., Braun, C.D., Allyn, A.J., Bograd, S.J., Brodie, S., Hazen, E.L., Kerney, A., Lezama-Ochoa, N., Mills, K.E., Pugh, D., Young-Morse, R., Lewison, R.L., 2024. Marine heatwaves redistribute pelagic fishing fleets. Fish Fish. 25 (4), 602–618. http://dx.doi.org/10.1111/faf.12828.
- Forget, G., Campin, J.-M., Heimbach, P., Hill, C.N., Ponte, R.M., Wunsch, C., 2015. ECCO version 4: an integrated framework for non-linear inverse modeling and global ocean state estimation. Geosci. Model. Dev. 8 (10), 3071–3104. http://dx. doi.org/10.5194/gmd-8-3071-2015.
- Frölicher, T.L., Fischer, E.M., Gruber, N., 2018. Marine heatwaves under global warming. Nature 560 (7718), 360–364. http://dx.doi.org/10.1038/s41586-018-0383-9.
- Gawarkiewicz, G., Plueddemann, A.J., 2020. Scientific rationale and conceptual design of a process-oriented shelfbreak observatory: the OOI Pioneer Array. J. Oper. Ocean. 13 (1), 19–36. http://dx.doi.org/10.1080/1755876X.2019.1679609.
- Gawarkiewicz, G., Chen, K., Forsyth, J., Bahr, F., Mercer, A.M., Ellertson, A., Fratantoni, P., Seim, H., Haines, S., Han, L., 2019. Characteristics of an advective marine heatwave in the middle atlantic bight in early 2017. Front. Mar. Sci. 6, http://dx.doi.org/10.3389/fmars.2019.00712.
- Gomes, D.G.E., Ruzicka, J.J., Crozier, L.G., Huff, D.D., Brodeur, R.D., Stewart, J.D., 2024. Marine heatwaves disrupt ecosystem structure and function via altered food webs and energy flux. Nat. Commun. 15 (1), 1988. http://dx.doi.org/10.1038/ s41467-024-46263-2.

- Gregory, C.H., Holbrook, N.J., Marshall, A.G., Spillman, C.M., 2024. Sub-seasonal to seasonal drivers of regional marine heatwaves around Australia. Clim. Dyn. http://dx.doi.org/10.1007/s00382-024-07226-x.
- Griffin, C., Beggs, H., Majewski, L., 2017. GHRSST compliant AVHRR SST products over the Australian region. Technical Report, Bureau of Meteorology, Melbourne, Australia. p. 152.
- Großelindemann, H., Ryan, S., Ummenhofer, C.C., Martin, T., Biastoch, A., 2022.
 Marine heatwaves and their depth structures on the northeast U.S. continental shelf. Front. Clim. 4, http://dx.doi.org/10.3389/fclim.2022.857937.
- Gruber, N., Boyd, P.W., Frölicher, T.L., Vogt, M., 2021. Biogeochemical extremes and compound events in the ocean. Nature 600 (7889), 395–407. http://dx.doi.org/10. 1038/s41586-021-03981-7.
- Haddock, S.H., Choy, C.A., 2024. Life in the midwater: The ecology of deep pelagic animals. Annu. Rev. Mar. Sci. 16 (1), 383–416. http://dx.doi.org/10.1146/annurevmarine-031623-095435.
- Hayashida, H., Matear, R.J., Strutton, P.G., 2020. Background nutrient concentration determines phytoplankton bloom response to marine heatwaves. Global Change Biol. 26 (9), 4800–4811. http://dx.doi.org/10.1111/gcb.15255.
- He, Q., Zhan, W., Feng, M., Gong, Y., Cai, S., Zhan, H., 2024. Common occurrences of subsurface heatwaves and cold spells in ocean eddies. Nature 1–7. http://dx.doi. org/10.1038/s41586-024-08051-2.
- Hernández-León, S., Koppelmann, R., Fraile-Nuez, E., Bode, A., Mompeán, C., Irigoien, X., Olivar, M.P., Echevarría, F., Fernández de Puelles, M.L., González-Gordillo, J.I., Cózar, A., Acuña, J.L., Agustí, S., Duarte, C.M., 2020. Large deep-sea zooplankton biomass mirrors primary production in the global ocean. Nat. Commun. 11 (1). 6048. http://dx.doi.org/10.1038/s41467-020-19875-7.
- Hersbach, H., Bell, B., Berrisford, P., Hirahara, S., Horányi, A., Muñoz-Sabater, J., Nicolas, J., Peubey, C., Radu, R., Schepers, D., Simmons, A., Soci, C., Abdalla, S., Abellan, X., Balsamo, G., Bechtold, P., Biavati, G., Bidlot, J., Bonavita, M., De Chiara, G., Dahlgren, P., Dee, D., Diamantakis, M., Dragani, R., Flemming, J., Forbes, R., Fuentes, M., Geer, A., Haimberger, L., Healy, S., Hogan, R.J., Hólm, E., Janisková, M., Keeley, S., Laloyaux, P., Lopez, P., Lupu, C., Radnoti, G., de Rosnay, P., Rozum, I., Vamborg, F., Villaume, S., Thépaut, J.-N., 2020. The ERA5 global reanalysis. Q. J. R. Meteorol. Soc. 146 (730), 1999–2049. http://dx.doi.org/10.1002/qj.3803.
- Hobday, A.J., Alexander, L.V., Perkins, S.E., Smale, D.A., Straub, S.C., Oliver, E.C., Benthuysen, J.A., Burrows, M.T., Donat, M.G., Feng, M., Holbrook, N.J., Moore, P.J., Scannell, H.A., Sen Gupta, A., Wernberg, T., 2016. A hierarchical approach to defining marine heatwaves. Prog. Oceanogr. 141, 227–238. http://dx.doi.org/10.1016/j.pocean.2015.12.014.
- Hobday, A.J., Oliver, E.C.J., Gupta, A.S., Benthuysen, J.A., Burrows, M.T., Donat, M.G., Holbrook, N.J., Moore, P.J., Thomsen, M.S., Wernberg, T., Smale, D.A., 2018. Categorizing and naming marine heatwaves. Oceanography 31 (2), 162–173. http://dx.doi.org/10.5670/oceanog.2018.205.
- Holbrook, N.J., Claar, D.C., Hobday, A.J., McInnes, K.L., Oliver, E.C.J., Gupta, A.S., Widlansky, M.J., Zhang, X., 2021. ENSO-driven ocean extremes and their ecosystem impacts. In: El Niño Southern Oscillation in a Changing Climate. American Geophysical Union (AGU), pp. 409–428.
- Holbrook, N.J., Goodwin, I.D., McGregor, S., Molina, E., Power, S.B., 2011. ENSO to multi-decadal time scale changes in East Australian Current transports and Fort Denison sea level: Oceanic Rossby waves as the connecting mechanism. Deep. Sea Res. Part II: Top. Stud. Ocean. 58 (5), 547–558. http://dx.doi.org/10.1016/j.dsr2. 2010.06.007
- Holbrook, N.J., Scannell, H.A., Sen Gupta, A., Benthuysen, J.A., Feng, M., Oliver, E.C.J., Alexander, L.V., Burrows, M.T., Donat, M.G., Hobday, A.J., Moore, P.J., Perkins-Kirkpatrick, S.E., Smale, D.A., Straub, S.C., Wernberg, T., 2019. A global assessment of marine heatwaves and their drivers. Nat. Commun. 10 (1), 2624. http://dx.doi. org/10.1038/s41467-019-10206-z.
- Hu, S., Li, S., Zhang, Y., Guan, C., Du, Y., Feng, M., Ando, K., Wang, F., Schiller, A., Hu, D., 2021. Observed strong subsurface marine heatwaves in the tropical western Pacific Ocean. Env. Res. Lett. 16 (10), 104024. http://dx.doi.org/10.1088/1748-9326/ac26f2.
- Huang, B., Yin, X., Carton, J.A., Chen, L., Graham, G., Liu, C., Smith, T., Zhang, H.-M., 2023. Understanding differences in sea surface temperature intercomparisons. J. Atmos. Ocean. Technol. 40 (4), 455–473. http://dx.doi.org/10.1175/JTECH-D-22-0081.1.
- Hughes, T.P., Anderson, K.D., Connolly, S.R., Heron, S.F., Kerry, J.T., Lough, J.M., Baird, A.H., Baum, J.K., Berumen, M.L., Bridge, T.C., Claar, D.C., Eakin, C.M., Gilmour, J.P., Graham, N.A.J., Harrison, H., Hobbs, J.-P.A., Hoey, A.S., Hoogenboom, M., Lowe, R.J., McCulloch, M.T., Pandolfi, J.M., Pratchett, M., Schoepf, V., Torda, G., Wilson, S.K., 2018. Spatial and temporal patterns of mass bleaching of corals in the Anthropocene. Science 359 (6371), 80–83. http://dx.doi.org/10.1126/science.aan8048.
- Hussey, N.E., Kessel, S.T., Aarestrup, K., Cooke, S.J., Cowley, P.D., Fisk, A.T., Harcourt, R.G., Holland, K.N., Iverson, S.J., Kocik, J.F., Mills Flemming, J.E., Whoriskey, F.G., 2015. Aquatic animal telemetry: A panoramic window into the underwater world. Science 348 (6240), 1255642. http://dx.doi.org/10.1126/science.1255642.
- Iglesias, I.S., Fiechter, J., Santora, J.A., Field, J.C., 2024. Vertical distribution of mesopelagic fishes deepens during marine heatwave in the California Current. ICES J. Mar. Sci. 81 (9), 1837–1849. http://dx.doi.org/10.1093/icesjms/fsae129.

- Jackson, J.M., Johnson, G.C., Dosser, H.V., Ross, T., 2018. Warming from recent marine heatwave lingers in deep British Columbia Fjord. Geophys. Res. Lett. 45 (18), 9757–9764. http://dx.doi.org/10.1029/2018GL078971.
- Jacox, M.G., Alexander, M.A., Bograd, S.J., Scott, J.D., 2020. Thermal displacement by marine heatwaves. Nature 584 (7819), 82–86. http://dx.doi.org/10.1038/s41586-020.2524.7
- Juza, M., Fernández-Mora, À., Tintoré, J., 2022. Sub-regional marine heat waves in the mediterranean sea from observations: Long-term surface changes, sub-surface and coastal responses. Front. Mar. Sci. 9, http://dx.doi.org/10.3389/fmars.2022. 785771
- Kauppi, L., Villnäs, A., 2022. Marine heatwaves of differing intensities lead to distinct patterns in seafloor functioning. Proc. R. Soc. B: Biol. Sci. 289 (1986), 20221159. http://dx.doi.org/10.1098/rspb.2022.1159.
- Kiss, A.E., Hogg, A.M., Hannah, N., Boeira Dias, F., Brassington, G.B., Chamberlain, M.A., Chapman, C., Dobrohotoff, P., Domingues, C.M., Duran, E.R., England, M.H., Fiedler, R., Griffies, S.M., Heerdegen, A., Heil, P., Holmes, R.M., Klocker, A., Marsland, S.J., Morrison, A.K., Munroe, J., Nikurashin, M., Oke, P.R., Pilo, G.S., Richet, O., Savita, A., Spence, P., Stewart, K.D., Ward, M.L., Wu, F., Zhang, X., 2020. ACCESS-OM2 v1.0: a global ocean–sea ice model at three resolutions. Geosci. Model. Dev. 13 (2), 401–442. http://dx.doi.org/10.5194/gmd-13.401.2020
- Köhn, E.E., Vogt, M., Münnich, M., Gruber, N., 2024. On the vertical structure and propagation of marine heatwaves in the Eastern Pacific. J. Geophys. Res.: Ocean. 129 (1), http://dx.doi.org/10.1029/2023JC020063.
- Lago, V., Roughan, M., Kerry, C., Knuckey, I., 2025. Fishing for ocean data in the east Australian current. Oceanography 38 (1), 67–71. http://dx.doi.org/10.5670/ oceanog.2025e105.
- Le Grix, N., Zscheischler, J., Laufkötter, C., Rousseaux, C.S., Frölicher, T.L., 2021. Compound high-temperature and low-chlorophyll extremes in the ocean over the satellite period. Biogeosciences 18 (6), 2119–2137. http://dx.doi.org/10.5194/bg-18-2119-2021.
- Lee, T., Hobbs, W.R., Willis, J.K., Halkides, D., Fukumori, I., Armstrong, E.M., Hayashi, A.K., Liu, W.T., Patzert, W., Wang, O., 2010. Record warming in the South Pacific and western Antarctica associated with the strong central-Pacific El Niño in 2009–10. Geophys. Res. Lett. 37 (19), http://dx.doi.org/10.1029/2010GL044865.
- Lee, E.Y., Lee, D.E., Park, Y.-G., Kang, H., Baek, H., 2023. The local stratification preconditions the marine heatwaves in the Yellow Sea. Front. Mar. Sci. 10, http: //dx.doi.org/10.3389/fmars.2023.1118969.
- Li, Z., Holbrook, N.J., Zhang, X., Oliver, E.C.J., Cougnon, E.A., 2020. Remote forcing of Tasman sea marine heatwaves. J. Clim. 33 (12), 5337–5354. http://dx.doi.org/ 10.1175/JCIJ-D-19-0641.1.
- Lo Bue, N., Best, M.M.R., Embriaco, D., Abeysirigunawardena, D., Beranzoli, L., Dewey, R.K., Favali, P., Feng, M., Heesemann, M., Leijala, U., Ó'Conchubhair, D., Scherwath, M., Scoccimarro, E., Wernberg, T., 2021. The importance of marine research infrastructures in capturing processes and impacts of extreme events. Front. Mar. Sci. 8, http://dx.doi.org/10.3389/fmars.2021.626668.
- Locarnini, R.A., Mishonov, A.V., Antonov, J.I., Boyer, T.P., Garcia, H.E., Baranova, O.K., Zweng, M.M., Paver, C.R., Reagan, J.R., Johnson, D.R., Hamilton, M., Seidov, D., Levitus, S., 2013. World ocean atlas 2013. NOAA Atlas NESDIS NOAA, Temperature NOAA Atlas NESDIS NOAA, 1.73,
- Malan, N., Roughan, M., Hemming, M., Ingleton, T., 2024. Quantifying coastal freshwater extremes during unprecedented rainfall using long timeseries multiplatform salinity observations. Nat. Commun. 15 (1), 424. http://dx.doi.org/10. 1038/s41467-023-44398-2.
- Manning, J., Pelletier, E., 2009. Environmental monitors on lobster traps (eMOLT): long-term observations of New England's bottom-water temperatures. J. Oper. Ocean. 2 (1), 25–33. http://dx.doi.org/10.1080/1755876X.2009.11020106.
- Manta, G., de Mello, S., Trinchin, R., Badagian, J., Barreiro, M., 2018. The 2017 record marine heatwave in the Southwestern Atlantic shelf. Geophys. Res. Lett. 45 (22), 12,449–12,456. http://dx.doi.org/10.1029/2018GL081070.
- Marin, M., Feng, M., Bindoff, N.L., Phillips, H.E., 2022. Local drivers of extreme upper ocean marine heatwaves assessed using a global ocean circulation model. Front. Clim. 4, http://dx.doi.org/10.3389/fclim.2022.788390.
- Martini, S., Haddock, S.H.D., 2017. Quantification of bioluminescence from the surface to the deep sea demonstrates its predominance as an ecological trait. Sci. Rep. 7 (1), 45750. http://dx.doi.org/10.1038/srep45750.
- McAdam, R., Masina, S., Gualdi, S., 2023. Seasonal forecasting of subsurface marine heatwaves. Commun. Earth Env. 4 (1), 1–11. http://dx.doi.org/10.1038/s43247-023-00892-5.
- McMahon, C.R., Roquet, F., Baudel, S., Belbeoch, M., Bestley, S., Blight, C., Boehme, L., Carse, F., Costa, D.P., Fedak, M.A., Guinet, C., Harcourt, R., Heslop, E., Hindell, M.A., Hoenner, X., Holland, K., Holland, M., Jaine, F.R.A., Jeanniard du Dot, T., Jonsen, I., Keates, T.R., Kovacs, K.M., Labrousse, S., Lovell, P., Lydersen, C., March, D., Mazloff, M., McKinzie, M.K., Muelbert, M.M.C., O'Brien, K., Phillips, L., Portela, E., Pye, J., Rintoul, S., Sato, K., Sequeira, A.M.M., Simmons, S.E., Tsontos, V.M., Turpin, V., van Wijk, E., Vo, D., Wege, M., Whoriskey, F.G., Wilson, K., Woodward, B., 2021. Animal Borne ocean sensors AniBOS An essential component of the global ocean observing system. Front. Mar. Sci. 8, http://dx.doi.org/10.3389/fmars.2021.751840.

- Meinen, C.S., Johns, W.E., Garzoli, S.L., van Sebille, E., Rayner, D., Kanzow, T., Baringer, M.O., 2013. Variability of the deep western boundary current at 26.5°N during 2004–2009. Deep. Sea Res. Part II: Top. Stud. Ocean. 85, 154–168. http: //dx.doi.org/10.1016/j.dsr2.2012.07.036.
- Ménesguen, C., Delpech, A., Marin, F., Cravatte, S., Schopp, R., Morel, Y., 2019.
 Observations and mechanisms for the formation of deep equatorial and tropical circulation. Earth Space Sci. 6 (3), 370–386. http://dx.doi.org/10.1029/2018EA000438.
- Merchant, C.J., Embury, O., Bulgin, C.E., Block, T., Corlett, G.K., Fiedler, E., Good, S.A., Mittaz, J., Rayner, N.A., Berry, D., Eastwood, S., Taylor, M., Tsushima, Y., Waterfall, A., Wilson, R., Donlon, C., 2019. Satellite-based time-series of seasurface temperature since 1981 for climate applications. Sci. Data 6 (1), 223. http://dx.doi.org/10.1038/s41597-019-0236-x.
- Mogen, S.C., Lovenduski, N.S., Dallmann, A.R., Gregor, L., Sutton, A.J., Bograd, S.J., Quiros, N.C., Di Lorenzo, E., Hazen, E.L., Jacox, M.G., Buil, M.P., Yeager, S., 2022. Ocean biogeochemical signatures of the North Pacific blob. Geophys. Res. Lett. 49 (9), http://dx.doi.org/10.1029/2021GL096938, e2021GL096938.
- Oliver, E.C.J., Benthuysen, J.A., Bindoff, N.L., Hobday, A.J., Holbrook, N.J., Mundy, C.N., Perkins-Kirkpatrick, S.E., 2017. The unprecedented 2015/16 Tasman Sea marine heatwave. Nat. Commun. 8 (1), 16101. http://dx.doi.org/10.1038/ncomms16101.
- Oliver, E.C., Benthuysen, J.A., Darmaraki, S., Donat, M.G., Hobday, A.J., Holbrook, N.J., Schlegel, R.W., Sen Gupta, A., 2021. Marine heatwaves. Annu. Rev. Mar. Sci. 13, 313–342. http://dx.doi.org/10.1146/annurev-marine-032720-095144.
- Oliver, E.C., Donat, M.G., Burrows, M.T., Moore, P.J., Smale, D.A., Alexander, L.V., Benthuysen, J.A., Feng, M., Sen Gupta, A., Hobday, A.J., Holbrook, N.J., Perkins-Kirkpatrick, S.E., Scannell, H.A., Straub, S.C., Wernberg, T., 2018. Longer and more frequent marine heatwaves over the past century. Nat. Commun. 9 (1), 1–12. http://dx.doi.org/10.1038/s41467-018-03732-9.
- Pedregosa, F., Varoquaux, G., Gramfort, A., Michel, V., Thirion, B., Grisel, O., Blondel, M., Prettenhofer, P., Weiss, R., Dubourg, V., Vanderplas, J., Passos, A., Cournapeau, D., Brucher, M., Perrot, M., Duchesnay, É., 2011. Scikit-learn: Machine learning in python. J. Mach. Learn. Res. 12 (85), 2825–2830.
- Pegliasco, C., Chaigneau, A., Morrow, R., 2015. Main eddy vertical structures observed in the four major Eastern Boundary Upwelling Systems. J. Geophys. Res.: Ocean. 120 (9), 6008–6033. http://dx.doi.org/10.1002/2015JC010950.
- Perkins, N.R., Monk, J., Soler, G., Gallagher, P., Barrett, N.S., 2022. Bleaching in sponges on temperate mesophotic reefs observed following marine heatwave events. Clim. Chang. Ecol. 3, 100046. http://dx.doi.org/10.1016/j.ecochg.2021.100046.
- Perkins-Kirkpatrick, S.E., King, A.D., Cougnon, E.A., Holbrook, N.J., Grose, M.R., Oliver, E.C.J., Lewis, S.C., Pourasghar, F., 2019. The role of natural variability and anthropogenic climate change in the 2017/18 Tasman Sea marine heatwave. Bull. Am. Meteorol. Soc. 100 (1), S105–S110. http://dx.doi.org/10.1175/BAMS-D-18-0116.1
- Piatt, J.F., Arimitsu, M.L., Thompson, S.A., Suryan, R., Wilson, R.P., Elliott, K.H., Sydeman, W.J., 2024. Mechanisms by which marine heatwaves affect seabirds. Mar. Ecol. Prog. Ser. 737, 1–8. http://dx.doi.org/10.3354/meps14625.
- Pilo, G.S., Holbrook, N.J., Kiss, A.E., Hogg, A.M., 2019. Sensitivity of marine heatwave metrics to ocean model resolution. Geophys. Res. Lett. 46 (24), 14604–14612. http://dx.doi.org/10.1029/2019GL084928.
- Prince, E.D., Goodyear, C.P., 2006. Hypoxia-based habitat compression of tropical pelagic fishes. Fisheries Oceanography 15 (6), 451–464. http://dx.doi.org/10.1111/j.1365-2419.2005.00393.x.
- Purcell, E.M., 1977. Life at low Reynolds number. Am. J. Phys. 45 (1), 3–11. http://dx.doi.org/10.1119/1.10903.
- Ren, X., Liu, W., Capotondi, A., Amaya, D.J., Holbrook, N.J., 2023. The Pacific Decadal Oscillation modulated marine heatwaves in the Northeast Pacific during past decades. Commun. Earth Env. 4 (1), 1–9. http://dx.doi.org/10.1038/s43247-023-00863-w.
- Reynolds, R.W., Rayner, N.A., Smith, T.M., Stokes, D.C., Wang, W., 2002. An improved in situ and satellite SST analysis for climate. J. Clim. 15 (13), 1609–1625. http://dx.doi.org/10.1175/1520-0442(2002)015<1609:AIISAS>2.0.CO;2.
- Reynolds, R.W., Smith, T.M., Liu, C., Chelton, D.B., Casey, K.S., Schlax, M.G., 2007. Daily high-resolution-blended analyses for sea surface temperature. J. Clim. 20 (22), 5473–5496. http://dx.doi.org/10.1175/2007JCLI1824.1.
- Ridgway, K.R., Ling, S.D., 2023. Three decades of variability and warming of nearshore waters around tasmania. Prog. Oceanogr. 215, 103046. http://dx.doi.org/10.1016/ j.pocean.2023.103046.
- Rodrigues, R.R., Taschetto, A.S., Sen Gupta, A., Foltz, G.R., 2019. Common cause for severe droughts in South America and marine heatwaves in the South Atlantic. Nat. Geosci. 12 (8), 620–626. http://dx.doi.org/10.1038/s41561-019-0393-8.
- Roemmich, D., Gilson, J., 2009. The 2004–2008 mean and annual cycle of temperature, salinity, and steric height in the global ocean from the Argo Program. Prog. Oceanogr. 82 (2), 81–100. http://dx.doi.org/10.1016/j.pocean.2009.03.004.

- Rogers-Bennett, L., Catton, C.A., 2019. Marine heat wave and multiple stressors tip bull kelp forest to sea urchin barrens. Sci. Rep. 9 (1), 15050. http://dx.doi.org/10. 1038/s41598-019-51114-v.
- Romero, E., Tenorio-Fernandez, L., Portela, E., Montes-Aréchiga, J., Sánchez-Velasco, L., 2023. Improving the thermocline calculation over the global ocean. Ocean. Sci. 19 (3), 887–901. http://dx.doi.org/10.5194/os-19-887-2023.
- Roughan, M., Hemming, M., Schaeffer, A., Austin, T., Beggs, H., Chen, M., Feng, M., Galibert, G., Holden, C., Hughes, D., Ingleton, T., Milburn, S., Ridgway, K., 2022. Multi-decadal ocean temperature time-series and climatologies from Australia's long-term National Reference Stations. Sci. Data 9 (1), 1–15. http://dx.doi.org/10.1038/s41597-022-01224-6.
- Ryan, S., Ummenhofer, C.C., Gawarkiewicz, G., Wagner, P., Scheinert, M., Biastoch, A., Böning, C.W., 2021. Depth structure of Ningaloo Niño/Niña events and associated drivers. J. Clim. 34 (5), 1767–1788. http://dx.doi.org/10.1175/JCLI-D-19-1020.1.
- Salinger, M.J., Diamond, H.J., Behrens, E., Fernandez, D., Fitzharris, B.B., Herold, N., Johnstone, P., Kerckhoffs, H., Mullan, A.B., Parker, A.K., Renwick, J., Scofield, C., Siano, A., Smith, R.O., South, P.M., Sutton, P.J., Teixeira, E., Thomsen, M.S., Trought, M.C.T., 2020. Unparalleled coupled ocean-atmosphere summer heatwaves in the New Zealand region: drivers, mechanisms and impacts. Clim. Change 162 (2), 485–506. http://dx.doi.org/10.1007/s10584-020-02730-5.
- Sallée, J.-B., Pellichero, V., Akhoudas, C., Pauthenet, E., Vignes, L., Schmidtko, S., Garabato, A.N., Sutherland, P., Kuusela, M., 2021. Summertime increases in upperocean stratification and mixed-layer depth. Nature 591 (7851), 592–598. http: //dx.doi.org/10.1038/s41586-021-03303-x.
- Salois, S.L., Hyde, K.J.W., Silver, A., Lowman, B.A., Gangopadhyay, A., Gawarkiewicz, G., Mercer, A.J.M., Manderson, J.P., Gaichas, S.K., Hocking, D.J., Galuardi, B., Jones, A.W., Kaelin, J., DiDomenico, G., Almeida, K., Bright, B., Lapp, M., 2023. Shelf break exchange processes influence the availability of the northern shortfin squid, , in the Northwest Atlantic. Fisheries Oceanography 32 (5), 461–478. http://dx.doi.org/10.1111/fog.12640.
- Scannell, H.A., Johnson, G.C., Thompson, L., Lyman, J.M., Riser, S.C., 2020. Subsurface evolution and persistence of marine heatwaves in the Northeast Pacific. Geophys. Res. Lett. 47 (23), http://dx.doi.org/10.1029/2020GL090548, e2020GL090548.
- Schaeffer, A., Roughan, M., 2017. Subsurface intensification of marine heatwaves off southeastern Australia: The role of stratification and local winds. Geophys. Res. Lett. 44 (10), 5025–5033. http://dx.doi.org/10.1002/2017GL073714.
- Schaeffer, A., Sen Gupta, A., Roughan, M., 2023. Seasonal stratification and complex local dynamics control the sub-surface structure of marine heatwaves in Eastern Australian coastal waters. Commun. Earth Env. 4 (1), 1–12. http://dx.doi.org/10. 1038/s43247-023-00966-4.
- Schlegel, R.W., Oliver, E.C.J., Hobday, A.J., Smit, A.J., 2019. Detecting marine heatwaves with sub-optimal data. Front. Mar. Sci. 6, http://dx.doi.org/10.3389/ fmars.2019.00737.
- Sen Gupta, A., Thomsen, M., Benthuysen, J.A., Hobday, A.J., Oliver, E., Alexander, L.V., Burrows, M.T., Donat, M.G., Feng, M., Holbrook, N.J., Perkins-Kirkpatrick, S., Moore, P.J., Rodrigues, R.R., Scannell, H.A., Taschetto, A.S., Ummenhofer, C.C., Wernberg, T., Smale, D.A., 2020. Drivers and impacts of the most extreme marine heatwave events. Sci. Rep. 10 (1), 19359. http://dx.doi.org/10.1038/s41598-020-75445-3.
- Silsbe, G.M., Malkin, S.Y., 2016. Where light and nutrients collide: The global distribution and activity of subsurface chlorophyll maximum layers. In: Glibert, P.M., Kana, T.M. (Eds.), Aquatic Microbial Ecology and Biogeochemistry: A Dual Perspective. Springer International Publishing, Cham, pp. 141–152.
- Simpson, J., Sharples, J., 2012. Introduction to the physical and biological oceanography of shelf seas. Cambridge University Press.
- Smale, D.A., Wernberg, T., Oliver, E.C.J., Thomsen, M., Harvey, B.P., Straub, S.C., Burrows, M.T., Alexander, L.V., Benthuysen, J.A., Donat, M.G., Feng, M., Hobday, A.J., Holbrook, N.J., Perkins-Kirkpatrick, S.E., Scannell, H.A., Sen Gupta, A., Payne, B.L., Moore, P.J., 2019. Marine heatwaves threaten global biodiversity and the provision of ecosystem services. Nat. Clim. Chang. 9 (4), 306–312. http://dx.doi.org/10.1038/s41558-019-0412-1.
- Smith, K.E., Aubin, M., Burrows, M.T., Filbee-Dexter, K., Hobday, A.J., Holbrook, N.J., King, N.G., Moore, P.J., Sen Gupta, A., Thomsen, M., Wernberg, T., Wilson, E., Smale, D.A., 2024. Global impacts of marine heatwaves on coastal foundation species. Nat. Commun. 15 (1), 5052. http://dx.doi.org/10.1038/s41467-024-49307-0
- Smith, K.E., Burrows, M.T., Hobday, A.J., Sen Gupta, A., Moore, P.J., Thomsen, M., Wernberg, T., Smale, D.A., 2021. Socioeconomic impacts of marine heatwaves: Global issues and opportunities. Science 374 (6566), http://dx.doi.org/10.1126/ science.abi3593.
- Sokolov, S., Rintoul, S.R., 2002. Structure of Southern Ocean fronts at 140°e. Physics and Biology of Ocean Fronts, J. Mar. Syst. Physics and Biology of Ocean Fronts, 37 (1), 151-184.http://dx.doi.org/10.1016/S0924-7963(02)00200-2,
- Solodoch, A., Stewart, A.L., Hogg, A.M., Morrison, A.K., Kiss, A.E., Thompson, A.F., Purkey, S.G., Cimoli, L., 2022. How does Antarctic bottom water cross the Southern Ocean? Geophys. Res. Lett. 49 (7), http://dx.doi.org/10.1029/2021GL097211, e2021GL097211. Publisher: John Wiley & Sons, Ltd.

- Sun, D., Li, F., Jing, Z., Hu, S., Zhang, B., 2023. Frequent marine heatwaves hidden below the surface of the global ocean. Nat. Geosci. 16 (12), 1099–1104. http: //dx.doi.org/10.1038/s41561-023-01325-w.
- Szuwalski, C.S., Aydin, K., Fedewa, E.J., Garber-Yonts, B., Litzow, M.A., 2023. The collapse of eastern Bering Sea snow crab. Science 382 (6668), 306–310. http://dx.doi.org/10.1126/science.adf6035.
- Testor, P., DeYoung, B., Rudnick, D.L., Glenn, S., Hayes, D., Lee, C., Pattiaratchi, C.B., Hill, K.L., Heslop, E., Turpin, V., Alenius, P., Barrera, C., Barth, J., Beaird, N., Becu, G., Bosse, A., Bourrin, F., Brearley, A., Chao, Y., Chen, S., Chiggiato, J., Coppola, L., Crout, R., Cummings, J., Curry, B., Curry, R., Davis, R., Desai, K., Di-Marco, S., Edwards, C., Fielding, S., Fer, I., Frajka-Williams, E., Gildor, H., Goni, G., Gutierrez, D., Hanson, S., Haugan, P., Hebert, D., Heiderich, J., Heywood, K.J., Hogan, P., Houpert, L., Huh, S., Inall, M.E., Ishii, M., Ito, S.-i., Itoh, S., Jan, S., Kaiser, J., Karstensen, J., Kirkpatrick, B., Klymak, J., Kohut, J., Krahmann, G., Krug, M., McClatchie, S., Marin, F., Mauri, E., Mehra, A., Meredith, M.P., Miles, T., Morell, J., Mortier, L., Nicholson, S., O'Callaghan, J., O'Conchubhair, D., Oke, P.R., Sanz, E.P., Palmer, M., Park, J., Perivoliotis, L., Poulain, P.-M., Perry, R., Oueste, B., Rainville, L., Rehm, E., Roughan, M., Rome, N., Ross, T., Ruiz, S., Saba, G., Schaeffer, A., Schonau, M., Schroeder, K., Shimizu, Y., Sloyan, B.M., Smeed, D., Snowden, D.P., Song, Y., Swart, S., Tenreiro, M., Thompson, A.F., Tintore, J., Todd, R.E., Toro, C., Venables, H., Waterman, S., Watlington, R., Wilson, D., 2019. OceanGliders: a component of the integrated GOOS. Front. Mar. Sci. 6, 422. http://dx.doi.org/10.3389/FMARS.2019.00422.
- Tsujino, H., Urakawa, S., Nakano, H., Small, R.J., Kim, W.M., Yeager, S.G., Danabasoglu, G., Suzuki, T., Bamber, J.L., Bentsen, M., Böning, C.W., Bozec, A., Chassignet, E.P., Curchitser, E., Boeira Dias, F., Durack, P.J., Griffies, S.M., Harada, Y., Ilicak, M., Josey, S.A., Kobayashi, C., Kobayashi, S., Komuro, Y., Large, W.G., Le Sommer, J., Marsland, S.J., Masina, S., Scheinert, M., Tomita, H., Valdivieso, M., Yamazaki, D., 2018. JRA-55 based surface dataset for driving ocean-sea-ice models (JRA55-do). Ocean. Model. 130, 79–139. http://dx.doi.org/10.1016/j.ocemod.2018.07.002.
- Vogt, L., Burger, F.A., Griffies, S.M., Frölicher, T.L., 2022. Local drivers of marine heatwaves: A global analysis with an earth system model. Front. Clim. 4, http: //dx.doi.org/10.3389/fclim.2022.847995.
- Walsh, J.J., 2013. On the nature of continental shelves. Elsevier.

- Welch, H., Savoca, M.S., Brodie, S., Jacox, M.G., Muhling, B.A., Clay, T.A., Cimino, M.A., Benson, S.R., Block, B.A., Conners, M.G., Costa, D.P., Jordan, F.D., Leising, A.W., Mikles, C.S., Palacios, D.M., Shaffer, S.A., Thorne, L.H., Watson, J.T., Holser, R.R., Dewitt, L., Bograd, S.J., Hazen, E.L., 2023. Impacts of marine heatwaves on top predator distributions are variable but predictable. Nat. Commun. 14 (1), 5188. http://dx.doi.org/10.1038/s41467-023-40849-y.
- Wernberg, T., Smale, D.A., Tuya, F., Thomsen, M.S., Langlois, T.J., de Bettignies, T., Bennett, S., Rousseaux, C.S., 2013. An extreme climatic event alters marine ecosystem structure in a global biodiversity hotspot. Nat. Clim. Chang. 3 (1), 78–82. http://dx.doi.org/10.1038/nclimate1627.
- Wirtz, K., Smith, S.L., Mathis, M., Taucher, J., 2022. Vertically migrating phytoplankton fuel high oceanic primary production. Nat. Clim. Chang. 12 (8), 750–756. http: //dx.doi.org/10.1038/s41558-022-01430-5.
- Wyatt, A.S.J., Leichter, J.J., Washburn, L., Kui, L., Edmunds, P.J., Burgess, S.C., 2023. Hidden heatwaves and severe coral bleaching linked to mesoscale eddies and thermocline dynamics. Nat. Commun. 14 (1), 25. http://dx.doi.org/10.1038/s41467-022-35550-5.
- Yang, B., Emerson, S.R., Peña, M.A., 2018. The effect of the 2013–2016 high temperature anomaly in the subarctic Northeast Pacific (the "Blob") on net community production. Biogeosciences 15 (21), 6747–6759. http://dx.doi.org/10.5194/bg-15-6747-2018.
- Young, J.W., Hunt, B.P.V., Cook, T.R., Llopiz, J.K., Hazen, E.L., Pethybridge, H.R., Ceccarelli, D., Lorrain, A., Olson, R.J., Allain, V., Menkes, C., Patterson, T., Nicol, S., Lehodey, P., Kloser, R.J., Arrizabalaga, H., Anela Choy, C., 2015. The trophodynamics of marine top predators: Current knowledge, recent advances and challenges. Deep. Sea Res. Part II: Top. Stud. Ocean. 170–187. http://dx.doi.org/10.1016/j.dsr2.2014.05.015.
- Yung, C.K., Holmes, R.M., 2023. On the contribution of transient diabatic processes to ocean heat transport and temperature variability. J. Phys. Oceanogr. 53 (12), 2933–2951. http://dx.doi.org/10.1175/JPO-D-23-0046.1.
- Zhang, Y., Du, Y., Feng, M., Hobday, A.J., 2023. Vertical structures of marine heatwaves. Nat. Commun. 14 (1), 6483. http://dx.doi.org/10.1038/s41467-023-42219-0.
- Zweng, M.M., Reagan, J.R., Antonov, J.I., Locarnini, R.A., Mishonov, A.V., Boyer, T.P., Garcia, H.E., Baranova, O.K., Johnson, D.R., Seidov, D., Biddle, M.M., Levitus, S., 2013. World ocean atlas 2013. NOAA atlas NESDIS, Salinity NOAA atlas NESDIS, 2, 74.http://dx.doi.org/10.7289/V5251G4D,